

# Assessing the State of Self-Supervised Human Activity Recognition using Wearables

HARISH HARESAMUDRAM, School of Electrical and Computer Engineering, Georgia Institute of Technology, USA

IRFAN ESSA, School of Interactive Computing, Georgia Institute of Technology, USA

THOMAS PLÖTZ, School of Interactive Computing, Georgia Institute of Technology, USA

The emergence of self-supervised learning in the field of wearables-based human activity recognition (HAR) has opened up opportunities to tackle the most pressing challenges in the field, namely to exploit unlabeled data to derive reliable recognition systems from only small amounts of labeled training samples. Furthermore, self-supervised methods enable a host of new application domains such as, for example, domain adaptation and transfer across sensor positions, activities etc. As such, self-supervision, i.e., the paradigm of 'pretrain-then-finetune' has the potential to become a strong alternative to the predominant end-to-end training approaches, let alone the classic activity recognition chain with explicit focus on designing feature representations for sensor data. Recently a number of contributions have been made that introduced self-supervised learning into the field of HAR, including, Multi-task self-supervision, Masked Reconstruction, CPC to name but a few. With the initial success of these methods, the time has come for a systematic inventory and analysis of the potential self-supervised learning has for the field. This paper provides exactly that. We assess the progress of self-supervised HAR research by introducing a framework that performs a multi-faceted exploration of model performance. We organize the framework into three dimensions, each containing three constituent criteria, and utilize it to assess state-of-the-art self-supervised learning methods in a large empirical study on a curated set of nine diverse benchmarks. This exploration leads us to the formulation of insights into the properties of these techniques and to establish their value towards learning representations for diverse scenarios. Based on our findings we call upon the community to join our efforts and to contribute towards shaping the evaluation of the ongoing paradigm change in modeling human activities from body-worn sensor data.

CCS Concepts: • Human-centered computing → Ubiquitous and mobile computing; Empirical studies in ubiquitous and mobile computing; • Computing methodologies → Machine learning.

Additional Key Words and Phrases: human activity recognition, representation learning, self-supervised learning

## 1 INTRODUCTION

Driven by the challenges of deriving effective human activity recognition systems from body-worn sensors (HAR), the recent years have seen a significant increase in interest towards learning unsupervised representations of movement data. While the collection of *annotated* data remains a challenge [41], the ubiquitous nature of the sensors themselves allows for the unobtrusive collection of large amounts of *unlabeled* data, which can subsequently be utilized to learn generic representations. For example, users can be given a smartwatch equipped with inertial measurement units (IMUs) in order to perform truly in-the-wild data collection of human behaviors. This practice of training first on large amounts of unlabeled data, followed by the fine-tuning on smaller quantities of labeled data has shown great promise for activity recognition applications [30, 31, 58–60, 65, 66].

These self-supervised approaches have the potential to alleviate challenges that come with limited annotations (incl. overfitting, and availability of less-complex modeling approaches only), and are therefore early proponents of the 'pretrain-then-finetune' paradigm shift. For example, in healthcare, collecting large amounts of data may be difficult, due to challenges with participant recruitment. This is compounded by the necessity to enlist healthcare

---

Authors' addresses: Harish Haresamudram, hharesamudram3@gatech.edu, School of Electrical and Computer Engineering, Georgia Institute of Technology, Atlanta, GA, USA; Irfan Essa, irfan@gatech.edu, School of Interactive Computing, Georgia Institute of Technology, Atlanta, GA, USA; Thomas Plötz, thomas.ploetz@gatech.edu, School of Interactive Computing, Georgia Institute of Technology, Atlanta, GA, USA.

professionals for annotation, which may incur high costs [34]. In such scenarios, self-supervised methods can jumpstart the training process by first learning relevant weights on large-scale background movement data.

Methods such as Multi-task self-supervision [58], Autoencoders [29], Masked reconstruction [30], and Contrastive Predictive Coding (CPC) [31] have been proposed, which aim towards learning generic representations for human activity recognition. Pre-training with self-supervision is first performed with unlabeled data, followed by fine-tuning of only a simple Multi-Layer Perceptron-based (MLP) classifier using annotations.

For these methods, model pre-training using unlabeled training data is typically either performed utilizing the same dataset as used for training the target activity recognition system—but without using label information—or with a larger background dataset such as Mobiact [8]. In either case, both the source and target data are rather similar by, for example, containing samples recorded from similar on-body positions of the movement sensors, and covering roughly the same activities. Therefore, this evaluation protocol is limited as it only studies one aspect of model performance, which makes it challenging to realize the conditions of effective performance as well as avenues of improvement for these approaches. To formulate a more well-rounded understanding of these approaches, and to inventory the current state of the field and its overall potential during this paradigm shift, we need to perform a multi-faceted, rigorous evaluation of these approaches in a variety of conditions and scenarios.

In this work, we conduct a large-scale empirical study ( $> 25k$  activity recognition runs) that evaluates contemporary self-supervised learning methods in HAR across multiple *dimensions* in an effort to "stress test" these methods, so as to shed light on the state-of-the-field. Our goal is to deepen the community's understanding of what these approaches learn, and under which conditions they perform best.

The evaluation is performed across three overarching dimensions:

- 1: Robustness to differing source and target conditions** – wherein the source and target scenarios have different data collection conditions, including sensor positions, activities, and sampling rates. Effective performance in this criterion indicates robustness in performance across varying target conditions.
- 2: Influence of dataset characteristics** – which studies the impact of the source and target characteristics on the activity recognition performance. Characteristics such as the class imbalance and quantity of unlabeled and labeled data detail how the setup of the datasets affects downstream recognition tasks.
- 3: Feature space characteristics** – post-hoc analysis of representations, such as similarity to supervised learning, linear separability, and implicit dimensionality, examines properties of learned representations.

We systematically evaluate self-supervised approaches for HAR [29–31, 58] on these criteria by first pre-training on the Capture-24 dataset [7, 21, 73], which contains wrist-worn accelerometry under free-living conditions for 151 participants over 2,500 hours. A standard MLP classifier [30, 31] is then used as the recognition backend. Through our study, we obtain insights into the workings of these methods under a variety of conditions and determine, for example, that they are not only effective across differing sensor positions, but also to activities not seen during pre-training. Furthermore, they are data efficient and robust to source dataset imbalances.

The main contributions of this paper are:

- We provide an overview of current wearables-based self-supervised human activity recognition research, which allows us to identify opportunities for novel applications and for further methodological research.
- We introduce an assessment framework comprising of three *dimensions*, which give us insights into when and where we can expect particular self-supervised approaches to be useful.
- We map out a research agenda for the evaluation of self-supervised methods in HAR, and call upon the community for a collaborative formulation of the evolved version of this assessment framework.

## 2 BACKGROUND AND MOTIVATION

Human activity recognition (HAR) is typically a five step process, as outlined in the activity recognition chain [57] – data collection, pre-processing, segmentation, feature extraction, and classification. Here, we focus on the fourth

This manuscript is under review. Please write to [harishkashyap@gatech.edu](mailto:harishkashyap@gatech.edu) for up-to-date information.

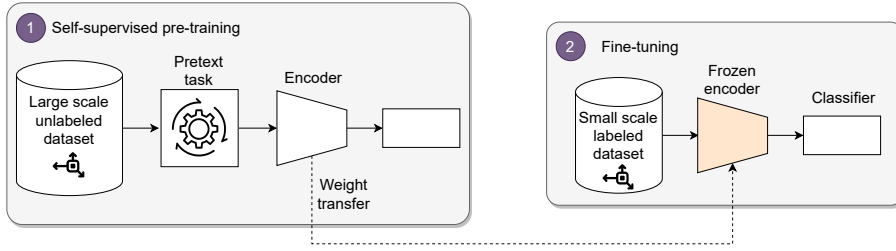


Fig. 1. Self-supervised learning comprises a two-stage process where pre-training is first performed with a large-scale unlabeled dataset. Subsequently, learned encoder weights are frozen and utilized for HAR on target, small labeled dataset.

step, which involves the extraction of relevant features for HAR. There are three main types of representations (or features) in human activity recognition: (i) statistical features: heuristics such as the mean, variance, entropy etc. [35, 52]; (ii) distribution-based features, which comprise the state-of-the-art for feature extraction, involving the inverse of the cumulative distribution function [28]; and (iii) learned features, consisting of dimensionality reduction techniques, supervised and unsupervised (incl. self-supervised) learning approaches [27, 29, 47, 58, 65].

In this work, we focus on methods that learn feature representations from unlabeled sample data. We perform an assessment of the progress of self-supervised human activity recognition with the goal to gather insights about the approaches and build an understanding of when they work well and where there are opportunities for improvement. We first discuss the progress made by unsupervised / self-supervised approaches towards learning effective representations for human activity recognition, followed by a brief discussion of prior works designed towards the analysis of self-supervised methods outside HAR and describe how we utilize a selection of them.

## 2.1 Self-Supervised Learning in Human Activity Recognition

Self-supervised learning involves utilizing domain expertise to define ‘pretext’ tasks, which require some semantic understanding. They are designed such that they capture relevant characteristics of the input data and by doing so learn weights that are beneficial for downstream recognition. These methods have shown great promise across many domains, including computer vision [22], natural language processing [16, 54, 55], and speech processing [11–13]. They follow the ‘pretrain-then-finetune’ training paradigm (see Fig. 1) and leverage potentially large quantities of unlabeled data for learning general representations.

Self-supervised learning was first explored for human activity recognition in a multi-task setting [58]. Saeed *et al.* [58] separately applied eight transformations, including adding noise, scaling, rotation, negation, flipping, permutation, time warping and channel-shuffling, with a probability of 50% in a multi-task setting to accelerometer data from mobile phones. The primary idea behind such a training scheme is that it allows for capturing core signal characteristics by learning to detect high-level semantics, sensor behavior under different device placements, time-shifting of the events, varying amplitudes, and robustness against sensor noise [58], thereby aiding in effective representation learning. The network comprises of a 1D convolutional encoder and task specific fully connected layers, and is trained to independently predict whether each transformation is applied or not. After the completion of the pre-training, the encoder layers are frozen and the classifier is evaluated for activity recognition, semi-supervised learning and transfer learning. It also contains feature space explorations including the representation similarity, tSNE plots [68], and saliency maps [62].

The use of transformer encoders for self-supervision was studied in [30]. The pretext task involves reconstructing the sensory data only at randomly masked timesteps of windowed accelerometer and gyroscope data from mobile phones. Ten percent of the timesteps are chosen randomly for masking, and data at those steps is set to zero before being input to the network. Mean squared error between the sensory data and reconstructed outputs at the masked timesteps is utilized to update network parameters. This approach seeks to learn useful

representations by capturing the local temporal dependencies in the sensory data, by reconstructing data at only the masked timesteps. Post training, the transformer encoder layers are frozen and only the multi-layer perceptron (MLP) classifier is optimized for activity recognition, and semi-supervised learning.

SelfHAR combined teacher-student self-training and multi-task self-supervision to increase internal and external diversity of training, thereby learning more generalizable features [65]. Knowledge distillation [33] is employed to first train the teacher on the labeled dataset. Subsequently, the learned teacher is used to pseudo-label the large-scale unlabeled dataset, and samples are filtered based on a threshold and top  $K$  samples are selected per class. The combined datasets are used for pre-training with multi-task self-supervision and the learned encoder weights are frozen and used for activity recognition on the original labeled dataset.

In contrast to previous works, SelfHAR also conducts experiments by using the large-scale, wrist-based unlabeled Fenland dataset [44, 48] and evaluating on the target datasets, which include those collected at the waist, thereby studying performance across sensor locations. There is also analysis looking into the effect of the composition of the source unlabeled dataset, where subsets are constructed based on the metabolic equivalents (MET) to obtain subsets with active, inactive, or balanced data. All subsets contained nearly the same number of samples and Tang *et al.* [65] find that balanced subsets lead to best downstream recognition performance.

The Contrastive Predictive Coding (CPC) framework was adopted and applied to human activity recognition in [31]. Windows of accelerometer and gyroscope data from mobile phones are encoded with a 1D convolutional encoder. A random timestep was chosen within the window and all encoded data prior to the timestep is summarized into a context vector by a gated recurrent unit (GRU) network [9]. Subsequently, this context vector was used to predict  $k$  future timesteps and the network is optimized using the InfoNCE loss [67]. The core idea behind CPC is that predicting only the next timestep needs the model to understand local variations, but predicting farther into the future is more difficult and requires the model to learn the slowly varying features, or the long term signal. Capturing such long term dependencies results in strong representation learning. The frozen encoder and GRU weights are used as feature extractor for activity recognition and semi-supervised learning.

Other self-supervised approaches in activity recognition include signal correspondence learning with the wavelet transform in a federated learning framework [59], utilizing eight auxiliary tasks for learning high-level features [60], contrastive learning for activity recognition in healthcare-based applications [66]. In most of the unsupervised and self-supervised approaches including Autoencoders, Multi-task self-supervision, Masked reconstruction, and CPC, the source and target datasets are typically the same for most experiments, albeit the pre-training does not use label information. In some cases, Mobiact [8] is used for pre-training instead as it is has the largest number of participants. Due to this, source and target conditions such as the activities covered (locomotion-style) and the sensor type (e.g., from mobile phones) and locations (the waist/trousers) are largely identical. Such an evaluation protocol only covers one aspect of measuring the model performance – which is under very similar training and testing conditions.

## 2.2 Analysis Methods for Understanding Self-Supervised Approaches

The burgeoning design and development of self-supervised approaches to leverage unlabeled data in domains like computer vision and natural language processing (NLP) has necessitated a body of work aimed at analyzing different properties of these methods. One of the approaches towards understanding representations involves the use of probing tasks, which have been successfully employed in NLP. Sentence embeddings were probed for interesting linguistic features such as the depth of the parse tree or if a sentence contains a specific word in [15]. Other works focus on lexical knowledge, being concerned with individual words rather than whole sentences [18, 70]. Analogous visual probing tasks were introduced in [4], along with a visual taxonomy. In contrast to vision which studies images, and natural language processing that tackles discrete sequences, wearable sensor data are continuous-valued time-series, thereby requiring modifications for applying some analyses protocols.

The effect of unlabeled dataset characteristics, such as class imbalance, on downstream performance was studied in [43, 74]. The authors demonstrate that self-supervised approaches are indeed more robust to source dataset imbalances (including long tailed distributions), thereby adding additional value to the utilization of self-supervision for initialization. The authors of [1] critically analyze self-supervised learning and study what percent of performance (compared to utilizing the full dataset) can be obtained by learning on augmented versions of a single image. As dataset imbalance is inherent to wearable sensing datasets, these analyses are of special importance and as such we utilize modified yet related versions of their protocols in our work.

Conditions of optimal performance for contrastive visual representation learning are studied in [14], including factors such as the pre-training domain, data quality, and task granularity. A similar strategy is adopted in [24] which explores scalability as a core tenet of self-supervised learning, by varying the scales of pre-training data, model capacity, and problem complexity across a series of visual tasks. As computational costs and model sizes are a prime concern for wearable sensing, we study the impact of quantity of pre-training data and the model capacity on performance in our work as well.

A systematic analysis of self-supervised vision transformers is conducted in [6], gathering insights into what information they contain, and show that the learned features are excellent kNN classifiers. It also underlines the importance of the various constituent steps towards effective performance. In a similar line of questioning, [38] takes a closer look at specifically the CNN architectures utilized for self-supervised learning via an empirical study. They observed that standard design recipes do not translate directly from end-to-end training to self-supervision with the number of filters being a significant factor. Finally, some approaches for post-hoc analysis of the learned representations include studying the similarity of the learned representations to the gold standard that is supervised learning [10, 20, 25], and understanding the intrinsic dimensionality of the representations [23, 71].

### 3 ASSESSMENT METHODOLOGY

The adoption of self-supervised learning has resulted in remarkable performance improvements in domains such as computer vision, natural language and speech processing. Particularly in the case of natural language processing, massive, high-quality datasets have been curated, facilitating the development of increasingly complex model architectures. With the introduction of increasingly effective models, the performance on established benchmarks saturated producing only minor improvements on old datasets and tasks. In order to push the field towards new frontiers, improved benchmarks were introduced such as, for example, General Language Understanding Evaluation (GLUE) [72] which focuses on natural language understanding (NLU), and Generation, Evaluation, and Metrics (GEM) [19] for natural language generation (NLG). Both benchmarks aggregate *multiple* diverse tasks under a single evaluation framework, thereby targeting many aspects of model performance concurrently. Interestingly, GEM eschews distilling the complex interplay between data, metrics and model outputs to a single value (like GLUE does) to an interactive result exploration system that presents performance across tasks [19]. Such a system facilitates more nuanced interpretations of the results while rejecting hill climbing prevalent in leaderboards.

In this work, we follow in the steps of GLUE and GEM by designing an evaluation framework specifically for HAR scenarios that comprises of a suite of diverse criteria organized in three dimensions. By evaluating on multiple criteria, we assess the generalizability of the methods and discover models that perform well across scenarios. Specifically, our framework is similar to GEM wherein we perform diverse evaluations, yet do not attempt to reduce the model performance across tasks into a combined value. Rather, the aim is to have nuanced analysis of model performance so as to gauge the progress of the domain and uncover areas of progress. The dimensions are summarized in Tab. 1 and detailed below.

Table 1. We define three types of evaluation criteria, each capturing a different part of the self-supervised learning pipeline.

Robustness to Differing Source and Target Conditions	Influence of Dataset Characteristics	Feature Space Characteristics
Performance across different sensor positions	Effect of dataset imbalance	Similarity to supervised representations
Performance for disparate activities	Quantity of unlabeled data required	Linear separability of the representations
Variations in the sampling rate	Performance under the availability of limited annotated data	Implicit dimensionality of the representations

### 3.1 Robustness to Differing Source and Target Conditions

This dimension captures the impact of differing source and target conditions such as the sensor locations, targeted activities, and sampling rates on activity recognition, thereby indicating the broad applicability of the methods under diverse settings. The criteria that form this dimension include:

**Performance across different sensor positions** – this criterion evaluates the applicability of self-supervised weights when the source data are collected from a different on-body position than the target domain. Effective performance across differing sensor locations allows for leveraging large scale unlabeled datasets – which are typically collected at the wrist (such as Capture-24 [7, 21, 73], Fenland [44, 48], and Biobank [17]), to jumpstart recognition for rarer leg-based activities such as classifying freeze of gait.

**Performance for disparate activities** – source and target domains can contain disparate activities; this criterion evaluates if these self-supervised methods can generalize to unseen activities during fine-tuning.

**Variations in the sampling rate** – target datasets can have different sampling rates compared to the source dataset, on which the pre-training was performed. This criterion examines whether the target sampling rate must match the source, i.e., if downsampling is required or not.

### 3.2 Influence of dataset characteristics

This dimension studies the impact of the characteristics, such as size of the unlabeled dataset required for pre-training, and the class imbalance on the activity recognition performance. Capturing such properties sheds light on optimal source and target domain setups for effective recognition. It comprises of the following criteria:

**Quantity of unlabeled data required** – considers data efficiency of the self-supervised methods. In particular, it looks at how many training users, or alternatively the number of training windows, are required for learning good pre-trained representations. Techniques that require smaller training sets are more advantageous as they result in reduced computational costs, a factor that is very important for wearables.

**Effect of dataset imbalance** – many wearable sensing datasets are inherently imbalanced, containing larger quantities of more easily performed activities such as walking or lying down, relative to physically demanding movements such as skipping with a rope. We observe such imbalances in free living as well, where sleep might comprise of 7-8 hours per day, but exercising might happen for much shorter durations (such as < 1 hour). Given that imbalance is inherent to the datasets, this criterion analyzes the impact of class imbalance in both source and target domains on activity recognition performance.

**Performance under the availability of limited annotated data** – in numerous target scenarios, the data collection and subsequent annotation maybe difficult due to cost or privacy issues. In such cases, approaches that can first pre-train on a different background dataset and subsequently adapt to a target scenario with limited labeling have great practical value. The situation is of great importance as it can occur during real-life deployment wherein users can be directed to provide minimal amounts of specific activity data for improving the model performance by adapting to user idiosyncrasies.

### 3.3 Feature Space Characteristics

This dimension involves the post-hoc analysis of the learned representations and allows us to gain insight of the properties of the features. The following criteria are involved in this dimension:

**Similarity to supervised learning** – compares the similarity of the self-supervised representations at each layer to an identical network trained end-to-end. This allows us to get an understanding of which approaches mimic the supervised features the best, and also the point in the network where the self-supervised weights diverge from end-to-end training.

**Linear separability of the representations** – analyzes whether the self-supervised methods create a feature space where data points are linearly separable. This gives insight into whether the learned features can enable a multitude of downstream tasks, and are not limited to specific ones that relate directly with the pre-training method.

**Implicit dimensionality of the representations** – captures the true capacity and redundancies in the representations learned by self-supervision [23]. Indicates the number of dimensions that the features can be reduced to, while still containing as much information as possible.

## 4 SETUP

We evaluate the performance of our approach on nine representative benchmark datasets. They have been chosen carefully to cover a wide range of application scenarios, including ranges of sensor positions, activities covered, and sampling rates employed for data recording. In what follows, we detail the experimental evaluation protocol, which includes descriptions of the: (i) Datasets used in our study; (ii) A brief overview of the self-supervised methods we study; (iii) Implementation details; and, (iv) Data pre-processing steps; (v) Evaluation metrics.

### 4.1 Datasets

In this work, we perform a large-scale empirical study on self-supervised approaches in human activity recognition, specifically focusing on a single accelerometer setup. This choice is motivated by the feasibility of only having a single wearable sensor for many scenarios. In order to facilitate the transfer of learned weights, we also utilize one accelerometer for the target datasets as well. A summary of the datasets used in this study is tabulated in Tab. 2 and discussed below.

**4.1.1 Capture-24.** Capture-24 [7, 21, 73] is a large-scale dataset containing recordings from 151 participants for approximately one day, resulting in a total of around 4,000 hours of recorded data.<sup>1</sup> The data is collected from a single Axivity AX3 wrist-worn activity tracker and is sampled at 100Hz. The annotation was performed with Vicon Autograph wearable cameras and Whitehall II sleep diaries, resulting in more than 2,500 hours of coarsely labeled data. The annotations are broken into > 200 fine-grained activities or 6 broadly defined activities such as sleep, sit-stand, mixed, walking, vehicle, and bicycling [73]. The authors also provide corresponding mapping between the more fine-grained labels and broad mappings for sleep monitoring, activity levels etc. In our setup, we randomly subset 90% of the participants for training, whereas the rest are used for validation. Thus, the training set comprises of 135 participants whereas the validation set consists of the remaining 16 participants. The dataset composition is imbalanced, with around 75% corresponding to either sleep or sit-stand, whereas bicycling comprises of only 0.78% of the train dataset windows, as shown in Fig.14 in the Appendix.

**4.1.2 Target datasets.** The aim of this study is to assess the self-supervised methods across multiple dimensions, so as to further our understanding of what they learn. In order to facilitate a broad evaluation of these approaches, we curate nine target datasets - with the goal of having a diverse collection of activities, number of participants, sensor locations, dataset sizes, and sensors utilized. We note that many of these datasets also contain other

<sup>1</sup>Downloaded from: <https://ora.ox.ac.uk/objects/uuid:99d7c092-d865-4a19-b096-cc16440cd001>

Table 2. Overview of the datasets used for our experimental evaluation. Capture-24 comprises the source dataset whereas the remaining nine datasets are the target. We chose three datasets per location—waist/trousers, wrist, and leg/ankle—covering a wide variety of activities and dataset sizes. Note that the sensor location in this table for Daphnet FoG is specified as ‘leg/ankle’ for uniformity; the actual location is on the shank, just above the ankle.

Dataset	Location	# Users	# Act.	Activities
Capture-24 [7, 21, 73]	Wrist	151	-	Free living
HHAR [64]	Wrist	9	6	Biking, sitting, going up and down the stairs, standing, and walking
Myogym [40]	Wrist	10	31	Seated cable rows, one-arm dumbbell row, wide-grip pulldown behind the neck, bent over barbell row, reverse grip bent-over row, wide-grip front pulldown, bench press, incline dumbbell flies, incline dumbbell press and flies, pushups, leverage chest press, close-grip barbell bench press, bar skullcrusher, triceps pushdown, bench dip, overhead triceps extension, tricep dumbbell kickback, spider curl, dumbbell alternate bicep curl, incline hammer curl, concentration curl, cable curl, hammer curl, upright barbell row, side lateral raise, front dumbbell raise, seated dumbbell shoulder press, car drivers, lying rear delt raise, null
Wetlab [61]	Wrist	22	9	Cutting, inverting, peeling, pestling, pipetting, pouring, stirring, transfer, null
Mobiact [8]	Waist/ Trousers	61	11	Standing, walking, jogging, jumping, stairs up, stairs down, stand to sit, sitting on a chair, sit to stand, car step-in, and car step-out
Motionsense [45]	Waist/ Trousers	24	6	Walking, jogging, going up and down the stairs, sitting and standing
USC-HAD [75]	Waist/ Trousers	14	12	Walking - forward, left, right, upstairs, and downstairs, running forward, jumping, sitting, standing, sleeping, and riding the elevator up and down
Daphnet FoG [2]	Leg/ Ankle	10	3	No freeze, freeze, null
MHEALTH [3]	Leg/ Ankle	10	13	Standing, sitting, lying down, walking, climbing up the stairs, waist bend forward, frontal elevation of arms, knees bending, cycling, jogging, running, jump front and back
PAMAP2 [57]	Leg/ Ankle	9	12	Lying, sitting, standing, walking, running, cycling, nordic walking, ascending and descending stairs, vacuum cleaning, ironing, rope jumping

sensors, such as gyroscopes or indeed accelerometers recording different sensor locations. Yet, we only consider accelerometer data collected at specific locations as detailed below, given that our focus is towards studying single sensor setups.

First, we consider target datasets collected at the wrist: (i) HHAR [64] that covers locomotion-style activities with data collected at the wrist and the waist using smartwatches and smartphones respectively; (ii) the Myogym dataset [40], studying short duration, fine-grained gym exercises such as dumbbell curls and rows, collected using the Myo armband; and (iii) Wetlab [61], which comprises of laboratory-based gestures and movements.

At the waist/trousers, we study two mobile phone based datasets - Mobiact [8] and Motionsense [45], and USC-HAD [75], which was recorded using the MotionNode platform. In each case, the activities studied typically include locomotion-style activities such as walking, running, lying down etc. Mobiact also contains short-term

transition activities such as stepping in and out of a car, whereas USC-HAD includes more static activities such as riding in the elevator.

Finally, the leg/ankle datasets include: (i) Daphnet [2], where the goal is to identify the freeze of gait symptoms in Parkinson’s disease; (ii) MHEALTH [3], which details a novel framework for the development of mobile health applications, and covers exercises in addition to locomotion activities; and, (iii) PAMAP2 [57] where we consider 12 activities of daily living such as domestic activities and sportive exercises (nordic walking, running etc.).

Apart from being recorded at different sensor locations and covering a diverse set of activities, they also contain a wide spread of participants, with six of the target datasets containing 10-15 participants. Mobiact is the most diverse with 61 participants, followed by Motionsense at 24. From an activity standpoint, many of these datasets cover locomotion activities such as walking, running, sitting etc whereas Myogym contains 31 fine-grained gym exercises. Lastly, most of the datasets have class imbalance (see Fig. 15 for reference) with Wetlab, Mobiact, MHEALTH and Myogym having the most severe class compositions.

## 4.2 Self-supervised HAR methods

In this work, we assess approaches belonging to the ‘pretrain-then-finetune’ paradigm wherein representations are first learned on a large-scale background dataset. Once trained, the models are freely usable for fine-tuning on diverse downstream scenarios, without requiring extra effort. Given a focus on such methods, we study the performance of four state-of-the-art self-supervised techniques (detailed descriptions are given in Sec. 2, and key HAR references are listed below):

**Multi-task Self-supervision** [58]: involves a multi-task setting and identifying whether signal transformations were applied or not. This was the earliest exploration into self-supervised learning for wearables and utilizes transformations targeted for accelerometry. It has also shown impressive performance under semi-supervised and transfer learning settings.

**Masked reconstruction** [30]: learns useful representations by reconstructing only masked out portions of the input windows, thereby leveraging local temporal dependencies. It has demonstrated strong recognition when data from both accelerometer and gyroscope are available.

**Contrastive Predictive Coding (CPC)** [31]: adopted and applied the contrastive predictive coding framework to wearable data, and makes use of long term temporal properties for effective representation learning by predicting multiple future timesteps. It performs successfully for activity recognition and semi-supervised learning, especially when multiple sensors are available.

**Autoencoder** [29, 58]: consists of reconstructing the entire input window of sensory data, through an encoder-decoder which are mirror images of each other. It has a simple setup and therefore typically functions as the baseline for many self-supervised methods.

Notably, we do not include SelfHAR [65] in our study as it employs self-training in conjunction with self-supervision. As described in Sec. 2.1, the teacher model trained on the labeled target dataset is utilized to pseudo-label and filter the source dataset, followed by self-supervised pre-training. Therefore, each target dataset results in its own pre-trained model, which limits generalizability and thus does not allow for the self-supervised transfer learning setup utilized in our study.

## 4.3 Implementation Details

We implemented all models using the Pytorch framework [49]. Here, we provide the hyperparameter search spaces for all self-supervised approaches and detail relevant information for each method.

As we are pre-training these techniques on a different dataset than studied in the original papers, we perform extensive hyperparameter tuning to obtain the best performance. We perform a random search over available combinations for Tab. 3 and 4, as it has been shown to be very effective compared to grid searches [5], while

also not consuming extensive computational resources. For Masked reconstruction, CPC, and Autoencoder, we randomly sample 20 sets of hyperparameter combinations during pre-training (the parameter spaces of which are detailed below), whereas for Multi-task self-supervision, we perform a grid search over the learning rates and L2 regularizations as the possible combinations are fewer than 20. During activity recognition, we randomly sample 50 hyperparameter combinations across the pre-trained parameters as well as the classification specific parameters such as the classifier learning rate and weight decay for each target dataset. For each combination, we perform 5-fold cross validation to obtain the average F1-score, which is more robust to the particular choice of participants in the splits, resulting in a total of 2,250 classifier runs per method across target datasets.<sup>2</sup> The best pre-training combination for each dataset is once again trained with five random seeds, and these trained models are utilized for five randomized classifier runs (using the same seeds as pre-training), in order to account for the effect of the choice of random seed. Subsequently, the mean and standard deviation of the F1-scores are reported in Tab. 3 and 4. Unless specified, all subsequent experiments utilize a similar setup of including both five-fold validation as well as five randomized runs, resulting in over 25k pre-training + classifier total runs. The best combination of parameters for each of these methods across all datasets has been tabulated in Tab. 6-10 in the Appendix, along with the best overall parameter setup in Tab. 11.

All pre-training and classification runs are trained for 50 epochs with the pre-training utilizing early stopping at 5 epochs. Similar to the original papers, the learning rate for classifiers for CPC, Masked reconstruction, and Autoencoder [29] reduces by a factor of 0.8 every 10 epochs.

**4.3.1 Multi-task Self-supervision.** The encoder architecture is identical to the original paper [58], which contained three 1D convolutional layers, having 32, 64 and 96 filters, with a kernel size of 24, 18 and 8 respectively. Each convolutional layer is followed by the ReLU activation function [46] as well as Dropout [63] with  $p=0.1$ . Global max pooling is applied after the last convolutional layer, thereby forming the encoder network. During pre-training, we perform a grid search over the learning rates  $\in \{1e-4, 3e-4, 5e-4\}$  and L2 regularization  $\in \{1e-4, 3e-4, 5e-4\}$ . For classification, the parameters include learning rates  $\in \{1e-4, 3e-4, 5e-4\}$  and L2 regularization  $\in \{1e-4, 3e-4, 5e-4\}$ .

**4.3.2 Masked Reconstruction.** Masked reconstruction is trained using a Transformer encoder [69] as detailed in the original paper [30]. The raw accelerometer data is transformed to 128 dimensional embeddings using a 1D convolutional layer. In order to inject a sense of time (or sequence) to the Transformer encoder, fixed sinusoidal embeddings are utilized and added to the embeddings for input to the encoder. The pre-training parameter space includes the number of layers  $\in \{2, 3, 4, 5, 6\}$ , the number of warmup steps in the Noam optimizer schedule  $\in \{20k, 40k, 60k, 80k, 100k\}$ , percentage of time steps masked  $\in \{10, 20, 30, 40, 50, 60, 70\}\%$ . The number of heads is set to 8, and the classifier learning rate is tuned  $\in \{1e-4, 5e-4, 1e-5\}$  with the L2 regularization  $\in \{0.0, 1e-4, 1e-5\}$ .

**4.3.3 CPC.** We utilize an identical setup to [31], which contains a convolutional encoder as well as a Gated Recurrent Unit (GRU) network [9]. The convolutional encoder comprises of 3 blocks, with each block containing a 1D convolutional network with reflect padding, followed by the ReLU [46] activation function and Dropout [63] with  $p=0.2$ . The blocks contain 32, 64, and 128 filters respectively, and the GRU has a size of 256 units, 2 layers and Dropout with  $p=0.2$ . Pre-training is performed over the following params: learning rate  $\in \{1e-3, 5e-4, 1e-4\}$ , L2 regularization  $\in \{0.0, 1e-4, 1e-5\}$ , kernel size  $\in \{3, 5\}$ , and batch size  $\in \{64, 128, 256\}$ . The classification utilizes learning rates  $\in \{1e-4, 5e-4, 1e-5\}$  and L2 regularization  $\in \{0.0, 1e-4, 1e-5\}$ .

**4.3.4 Autoencoder.** The encoder for this method is identical to the convolutional encoder of CPC [31] (detailed above), and contains three convolutional blocks. The decoder is the mirror opposite of the encoder, also consisting

<sup>2</sup>50 combinations  $\times$  5 folds  $\times$  9 datasets

of three convolutional blocks but with reducing number of filters, 128, 64, and 32, respectively. The pre-training parameters include learning rate  $\in \{1e-3, 5e-4, 1e-4\}$ , weight decay  $\in \{0.0, 1e-4, 1e-5\}$ , and kernel size  $\in \{3, 5, 7, 9, 11\}$ . For classification, the learning rates  $\in \{1e-4, 5e-4, 1e-5\}$  and L2 regularization  $\in \{0.0, 1e-4, 1e-5\}$ .

**4.3.5 MLP Classifier.** All self-supervised methods are evaluated on a common backend network, identical to the classifier described in [30, 31]. After the pre-training is complete, the encoder weights are frozen and only the classifier network is updated via the cross entropy loss. It consists of three linear layers of 256, 128 and  $num\_classes$  units respectively. Between each layer, batch normalization [36], the ReLU activation function, and Dropout with p=0.2 are applied consecutively.

**4.3.6 DeepConvLSTM.** We implement the DeepConvLSTM architecture detailed in [47], which contains four 2D convolutional layers containing 64 filters and kernel size of  $5 \times 1$ . This is followed by a LSTM network of 2 layers and 128 units, followed by a linear classifier layer. The parameter search is performed over learning rate  $\in \{1e-3, 5e-4, 1e-4\}$ , and weight decay  $\in \{0.0, 1e-4, 1e-5\}$ . In addition, the learning rate is reduced by a factor of 0.8 every 10 epochs.

#### 4.4 Data Preparation

We utilize raw accelerometer data from the source and all target datasets. We perform no filtering or denoising on the datasets, as deep networks have shown powerful capabilities towards learning from raw data itself [42].

We downsample the large-scale Capture-24 dataset to 50 Hz as it reduces the computational load for pre-training. Additionally, this is also the lowest native sampling rate in the target datasets. We reduced the sampling frequency of all target datasets to match 50 Hz.<sup>3</sup> The normalization is performed at a per-channel level such that the train split has zero mean and unit variance. The means and variances obtained for the train split are utilized for normalizing the validation split.

The window size is set to 2 seconds to ensure that any randomly picked window can reasonably capture both longer duration activities (such as standing or walking), as well as more short-term activities including gestures and gym exercises. For Capture-24, the overlap is set to zero for efficiency reasons because it is a very large dataset, whereas the target datasets have an overlap of 50% as per usual in HAR applications.

We setup five-fold cross validation for each target dataset. Each fold consists of 20% of randomly chosen users comprising the test split, whereas the remaining 80% of users are once again separated into the train and validation splits at a 80:20 ratio. Overall, every participant appears exactly once as part of the validation and test splits and pairwise correlations of analysis windows are effectively eliminated through the user-based splits [26]. Finally, the means and variances obtained during the normalization of the Capture-24 training set are applied to the target datasets in order to match the dataset statistics.

#### 4.5 Performance Metric

We utilize the test set mean F1-score (i.e., macro F1-score) as the main metric to evaluate performance. This is motivated by the substantial class imbalance present in the target datasets (see Fig. 15 for reference), and thus we require a metric that is resistant to such bias in the class distribution [53]. The accuracy and weighted F1-score are not utilized as they are affected by the skewed class distributions, whereas the unweighted mean F1-score, while not ideal, is a reasonable strategy [50].

The mean F1-score is computed using:

$$F_m = \frac{2}{|c|} \sum_c \frac{prec_c \times recall_c}{prec_c + recall_c} \quad (1)$$

<sup>3</sup>The Daphnet FoG dataset was originally captured at 64 Hz and is therefore not downsampled as the sampling rates are comparable.

where  $|c|$  is the number of classes, and  $prec_c$  and  $recall_c$  are the precision and recall for each class respectively.

## 5 RESULTS

In this section, we systematically explore the performance of the self-supervised approaches as measured using the dimensions presented in Sec. 3. The goal of our exploration is to perform a well-rounded assessment of these methods to shed light on the avenues of improvement as well as identifying optimal conditions for effective performance across application boundaries. First, we evaluate the performance of self-supervised approaches when source and target conditions are not identical, followed by the analysis into how source and target dataset properties affect downstream performance. Finally, we assess the learned representations via an exploration of the feature space, which will further our understanding of representations learned via self-supervision.

### 5.1 Robustness to Differing Source and Target Conditions

For many applications of wearables, the collection of large-scale labeled datasets may be difficult or downright impossible due to privacy or cost reasons. In such cases, it may be possible, however, to leverage datasets collected under different conditions (such as sensor locations or targeted activities) by first pre-training to learn useful weights, and subsequently fine-tuning to the specific smaller scale dataset/application.

This dimension of our evaluation measures the efficacy of such a training process whereby the utility of using a completely disparate dataset/application for pre-training is measured. We begin by evaluating the effect of sensor positions on the recognition performance, followed by studying how variation in the activities recorded between the source and target datasets affects activity recognition. Lastly, we investigate whether target datasets with higher native sampling rates need to be downsampled to match the pre-training frequency. Overall, these criteria shed light on how universal the self-supervised representation learning methods are, as this evaluation stress tests the limits of the methods' transfer capabilities.

**5.1.1 Performance across different sensor positions.** As the Capture-24 dataset is collected at the wrist, we evaluate the learned weights at other on-body locations including the waist/trousers (where people often carry their smartphones), and the leg – where sensors may be placed to target applications such as detecting freeze of gait in Parkinson's disease or for measuring fitness. The DeepConvLSTM network [47] serves as our supervised baseline. All layers of the network are trained using the target dataset labels. For the self-supervised methods, we only fine-tune the weights of the multi-layer perceptron (MLP) classifier with the target dataset labels whereas the encoder is pre-trained without any annotations. The results of this evaluation are detailed in Tab. 3.

For the waist-based Motionsense dataset, we note that both Multi-task self supervision as well as CPC perform comparably to DeepConvLSTM. We see a similar trend for the Daphnet FoG dataset where the performance of DeepConvLSTM is close to the performance of *all* self-supervised approaches. Multi-task self-supervision shows a small improvement over DeepConvLSTM on both MHEALTH and USC-HAD while CPC perform similarly. On PAMAP2 however, we see significant gains of Multi-task self supervision (~7% over the mean) and Masked reconstruction (~4% over the mean) over DeepConvLSTM.

Only in the case of Mobiact, we observe that DeepConvLSTM significantly outperforms the self-supervised methods, increasing by over 10% against CPC, which is the best performing method in this case. The overall trend is that transferring weights from the wrist to the waist results in worsened performance (Mobiact) or comparable/only slightly better performance (Motionsense and USC-HAD). This is especially the case for Masked reconstruction, which has high test set F1-scores for the leg-based datasets while performing poorly on the waist-based data. In comparison, transferring from the wrist to leg results in comparable performance (Daphnet FoG) or considerable gains (MHEALTH and Pamap2). This is can be reasoned by the fact that many activities such as walking, running etc., which are a part of the MHEALTH and PAMAP2 datasets, have tandem motion between the wrist and the leg. We posit that this results in effective representations via self-supervision.

Table 3. The representation learning performance of the self-supervised approaches across differing sensor positions. compared against supervised learning. We perform 5-fold cross validation across 5 randomized runs and report the mean and standard deviation.

Method	Waist			Leg		
	Mobiact	Motionsense	USC-HAD	Daphnet FOG	MHEALTH	PAMAP2
DeepConvLSTM	82.21 ± 0.69	84.56 ± 0.85	53.64 ± 0.51	53.68 ± 2.58	45.91 ± 0.89	51.22 ± 1.91
Multi-task self. sup	69.71 ± 2.03	83.18 ± 1.26	56.63 ± 1.34	54.16 ± 1.12	48.05 ± 1.05	58.49 ± 3.03
Masked Recons.	54.17 ± 1.38	75.72 ± 1.88	45.09 ± 0.92	52.51 ± 1.01	47.04 ± 0.61	55.12 ± 0.96
CPC	72.91 ± 0.99	84.74 ± 1.14	51.37 ± 2.43	51.16 ± 1.0	45.49 ± 1.27	52.24 ± 1.98
Autoencoder	68.69 ± 0.56	80.7 ± 1.66	51.32 ± 2.16	53.05 ± 0.85	39.2 ± 1.58	56.88 ± 2.04

On the whole, self-supervised methods perform comparably, if not better, to the supervised baseline (DeepConvLSTM) even though the source location is at the wrist, whereas the target datasets were collected at the waist/leg. This result is encouraging as it allows practitioners to utilize large-scale movement datasets (which are typically collected at the wrist, e.g., through smartwatches) for fine-tuning on waist- or leg-based applications.

**5.1.2 Performance for disparate activities.** This criterion evaluates the effect of variations in the activities covered by the source and target datasets on the self-supervised learning performance. For example, sufficient quantities of labeled data are difficult to obtain for many medical applications of wearable sensing. In such cases, *would it be possible to leverage another dataset with completely disjointed activities for pre-training?*

For this analysis, we consider the datasets whose activities are at least partially not contained in the source dataset across the wrist and leg sensor positions. For example, the Myogym dataset comprises of specific gym exercises under various orientations (seated, bent over, on stomach, on an incline etc.), some of which may not have been performed by the participants of Capture-24. Similarly, the Wetlab dataset contains laboratory experiments, which are typically not performed in day-to-day living.

Compared to HHAR, which contains locomotion-style activities and is most similar to Capture-24 with regards to activities covered, *all* self-supervised methods show comparable if not better performance over the supervised baseline. Myogym contains gym exercises including curls, raises, and dips collected at the wrist. As such, CPC performs comparably to DeepConvLSTM whereas Multi-task self-supervision demonstrates improvements of ~2% over the mean. Wetlab is an exception wherein DeepConvLSTM clearly outperforms the self-supervised methods by a considerable margin.

MHEALTH and PAMAP2 both have activities that can be expected in daily living, albeit they are collected at the leg/ankle, rather than the wrist. In each case, self-supervision results in significant improvements over DeepConvLSTM for PAMAP2 (>7% over the mean) and minor improvements for MHEALTH (~2% over the mean). It is interesting to note that the self-supervised approaches perform comparably to DeepConvLSTM on the Daphnet FoG dataset, which contains freeze of gait symptoms for patients with Parkinson’s Disease. The comparable performance of all self-supervised methods on such rarely accessible medical data demonstrates their generalization capacity and their value towards utilization in conditions where labeled data maybe difficult to obtain. All in all, self-supervised methods trained on daily living data from Capture-24 can generalize well to unseen classes including freeze of gait and gym-based exercises.

**5.1.3 Variations in the sampling rate.** The sampling rate of the sensors must be taken in consideration for real-world deployment of wearable systems. A low sampling rate conserves computational resources and energy, but trades off against missing relevant signal details that may be vital to discriminating between activities [37].

In our study, the target datasets are often recorded at higher rates, e.g., the Mobiact dataset was recorded at 200 Hz whereas PAMAP2 was collected at 100 Hz, whereas Capture-24 was downsampled to 50 Hz. Therefore, we determine if target datasets must be downsampled for matching the sampling rates, and if it is detrimental if

Table 4. The representation learning performance of the self-supervised approaches across different source and target activities, compared against supervised learning. We perform 5-fold cross validation across 5 randomized runs and report the mean and standard deviation.

Method	Wrist			Leg		
	HHAR	Myogym	Wetlab	Daphnet FOG	MHEALTH	PAMAP2
DeepConvLSTM	54.39 $\pm$ 2.28	39.9 $\pm$ 1.05	31.0 $\pm$ 0.68	53.68 $\pm$ 2.58	45.91 $\pm$ 0.89	51.22 $\pm$ 1.91
Multi-task self. sup	57.51 $\pm$ 1.9	42.31 $\pm$ 2.37	23.35 $\pm$ 0.66	54.16 $\pm$ 1.12	48.05 $\pm$ 1.05	58.49 $\pm$ 3.03
Masked Recons.	55.04 $\pm$ 2.58	25.29 $\pm$ 0.68	21.23 $\pm$ 0.31	52.51 $\pm$ 1.01	47.04 $\pm$ 0.61	55.12 $\pm$ 0.96
CPC	58.1 $\pm$ 1.06	39.89 $\pm$ 0.98	24.16 $\pm$ 0.48	51.16 $\pm$ 1.0	45.49 $\pm$ 1.27	52.24 $\pm$ 1.98
Autoencoder	54.25 $\pm$ 2.04	35.45 $\pm$ 0.49	25.75 $\pm$ 1.03	53.05 $\pm$ 0.85	39.2 $\pm$ 1.58	56.88 $\pm$ 2.04

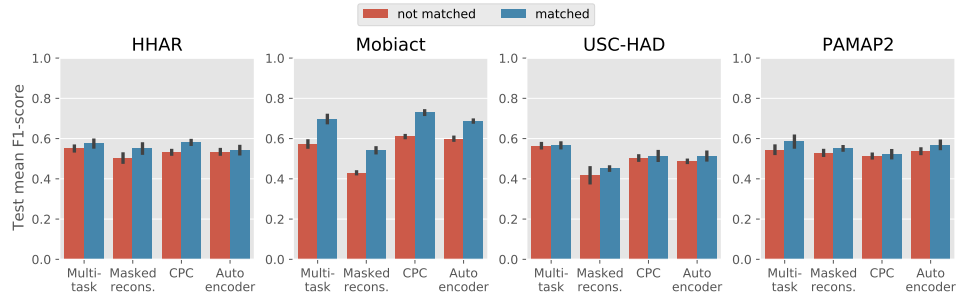


Fig. 2. Studying the effect of mismatches in sampling rates of the target datasets to the source dataset: we utilize the best performing models as detailed in Tab. 3 and 4 and choose target datasets whose native sampling rate is greater than Capture-24’s recording sampling rate. We perform five randomized runs include the pre-training and classification. The mean values of the target test set F1-scores are plotted along with the standard deviation for the five runs. For the chosen target datasets, the native sampling rate is either 100 or 200 Hz, thereby utilizing half or a quarter of the original pre-training window duration (two seconds). We observe a considerable drop in performance, especially for the Mobiact dataset (200 Hz). As the evaluation window duration is 1/4 times the pre-training, we observe a considerable drop in performance.

the target datasets’ native sampling rates are utilized. Effective performance even when downsampled results in the conservation of the scarce resources available during deployment. As such, *what is the effect of not matching the target frequency to the source dataset frequency?* After the pre-training is complete, we compare the activity recognition performance on the target datasets with and without downsampling (shown in Fig. 2).

We observe that all self-supervised methods perform poorly on Mobiact when the sampling rate is not matched to 50 Hz. As the original sampling rate of Mobiact is 200Hz, a window size of 100 samples is 0.5 seconds of data, whereas the pre-training consisted of two seconds of data, thereby resulting in degraded performance. The other datasets were recorded at 100 Hz and the reduction in performance occurs to a smaller extent for some of the self-supervised methods. Masked reconstruction struggles the most, likely because it depends on surrounding context to predict the missing values. If the target dataset is sampled at a different rate, the context looks different than what is seen during pre-training. Surprisingly, Multi-task self-supervision is affected to a significant extent (see Mobiact and PAMAP2) despite having access to a time warping augmentation during pre-training. Overall, it is preferable to match the source dataset sampling rates as it different sampling rates result in reduced performance. The degradation in the F1-score exacerbates with higher frequencies.

## 5.2 Influence of Dataset Characteristics

The previous dimension evaluated the quality of representations when the target dataset conditions differed from the pre-training setup. We established that pre-training on a large-scale dataset collected at the wrist has a

positive impact on the target activity recognition, even when the sensor locations are different or if the activities are not covered during pre-training. A natural extension of the first dimension is to analyze how properties of the datasets, e.g., the number of participants and data collected, affect the downstream recognition performance. First, we study the quantity of unlabeled data required for learning effective representations. Subsequently, we look at how the class distribution of the source and target datasets impacts the representations learned via self-supervision. Finally, we study the performance of these methods when there is limited labeled target data available for fine-tuning. Put together, these criteria illuminate the ideal compositions of the datasets, and if extra care must be taken during unlabeled data collection in order to produce the most useful representations possible.

**5.2.1 Quantity of the unlabeled data required.** This criterion evaluates the data efficiency of the self-supervised methods and determines how many participants and what quantities of data overall are necessary for robust learning. Methods, which are effective without requiring many users or hours of data are preferable [51]. We study the relation between the amount of unlabeled data and the downstream recognition performance from two perspectives: (i) the number of training participants required; and, (ii) the number of training windows (across all training users) necessary for effective pre-training.

*Effect of the number of training users on activity recognition.* Fig. 3 details the recognition performance relative to the number of training subjects used for pre-training. Out of the 135 training subjects of Capture-24, we randomly sample  $\{1, 5, 10, 25, 50, 100\}\%$  of the participants for pre-training, which corresponds to  $\{1, 6, 13, 33, 67, 135\}$  individuals. We perform three randomized runs, including choosing training subject(s), pre-training, and classification on the target datasets. We plot the mean and standard deviation of the test set mean F1-score obtained after five-fold validation.

For all target datasets, we observe that utilizing only one subject for pre-training results in poorer performance. This is especially true for Masked Reconstruction, which utilizes a large transformer encoder and thus requires more data. Adding more subjects improves performance until 50% of the participants are used for pre-training. Multi-task self-supervision and CPC benefit from larger number of participants but there is generally no significant gain between using 25% of the subjects over utilizing the entire training set. Contrary to the other approaches, the Autoencoder does not improve with the addition of further participants. For example, in the case of datasets such as MHEALTH, Myogym, USC-HAD and Mobiact, the best performance is obtained when only one random participant is for pre-training. Thus, the self-supervised methods such as Multi-task self-supervision, CPC, and Autoencoder do not require the entire training set (135 participants) for best performance, and can be trained for increased efficiency with fewer participants without much loss in performance.

*Effect of the number of training windows on activity recognition.* For data collection, it may not be possible to recruit a large set of participants who are willing to wear sensor(s) for long periods of time. It may be more practical to record data for shorter periods of time in free-living or indeed lab conditions. In this experiment, we study the feasibility of collecting a smaller yet diverse (participant-wise) unlabeled dataset with a goal of pre-training for activity recognition.

The Capture-24 dataset contains 135 participants in the training set, resulting in around 4.1 million non-overlapping windows. We create smaller subsets of training data by randomly sub-sampling windows in increasing orders of magnitude of percentages consisting of  $\{0.01, 0.1, 1, 10, 50, 100\}\%$  of the training windows from **all** participants and pre-train self-supervised models, whereas the validation set of Capture-24 remains untouched. Three randomized runs of pre-training (incl. the randomized subsampling) and classification are performed, and the mean and standard deviation of five-fold test set F1-scores are plotted in Fig. 4.

As can be expected, utilizing only 0.01% (i.e., ~410) of the training windows results in significantly worse activity recognition. This is especially clear for CPC, which shows a near monotonic increase with the addition of more training windows. The Multi-task method also performs similarly, getting higher F1-scores with increasing

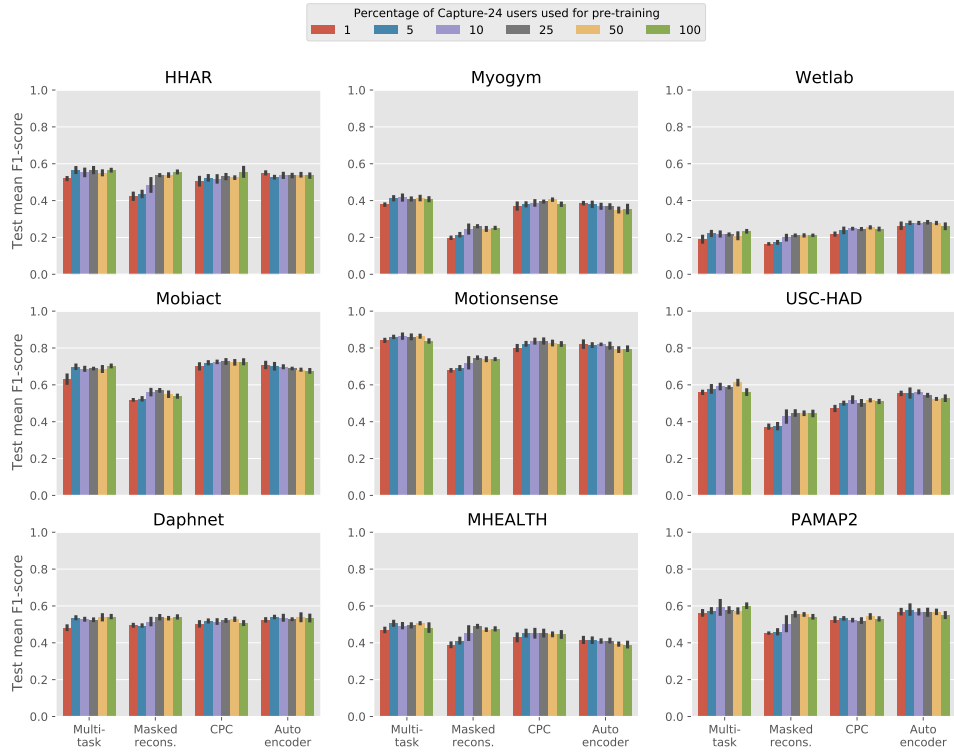


Fig. 3. Studying the effect of the number of training users on the downstream performance: we utilize the best overall hyperparameter combination (see Tab. 11) and pre-train with the respective approaches while using a varying number of training participants. The validation users for Capture-24 are untouched. We perform three randomized runs from choosing the training participants to pre-training, and finally activity recognition. The mean of the target test set F1-scores is plotted along with the standard deviation for three random runs. We observe that in most cases, utilizing fewer users results in comparable if not better performance to using the entirety of the training set (which is 135 users). Surprisingly, using data from just one user does not result in poor performance; rather, the performance is close to utilizing all available training data.

quantities of training windows. Masked Reconstruction demonstrates a sharp jump in performance between using 1% and 10% of the windows while the F1-score steadies beyond that. It is interesting to see that the Autoencoder shows the best performance using just  $\sim 410$  windows on some datasets (such as Myogym, USC-HAD, Mobiact) etc. It is able to learn effective representations with such limited data, showing a similar trend to Fig. 3 wherein the best results were obtained while training one user. As a general trend, we observe that the self-supervised methods obtain comparable if not better performance when utilizing only 10% (or  $\sim 400k$ ) of training windows.

**5.2.2 Effect of the dataset imbalance on performance.** Wearables-based movement datasets tend to be imbalanced, often containing considerably more samples of activities that either occur more naturally or can be performed easily, relative to more physically strenuous or rarely occurring activities. For example, datasets recorded in free-living conditions might contain 7-8 hours of sleep data but contain substantially shorter durations for exercise or commutes. Due to this, we study the impact of the dataset composition on activity recognition performance, for both the source and target datasets.

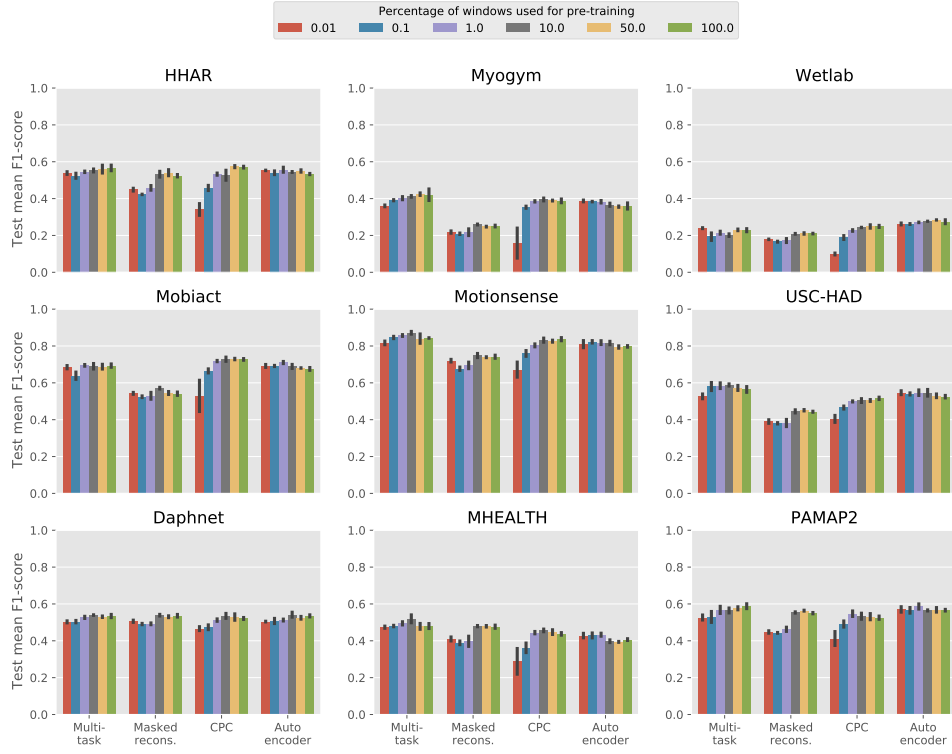


Fig. 4. Studying the effect of the number of training windows on the downstream performance: we utilize the best overall hyperparameter combination (see Tab. 11), and pre-train with the respective approaches while using a varying number of training windows. The training windows are sampled randomly from **all** training participants, while the validation data for Capture-24 are untouched. We perform three randomized runs for choosing the training windows, performing pre-training and activity recognition, and plot the mean of the target test set F1-scores along with the standard deviation. We note that excellent performance can be obtained while using 10% of the training windows, and in some cases using as few as 1% of the training windows. Using a smaller training is advantageous as it can allow for reduced computation costs and for more comprehensive hyperparameter searching.

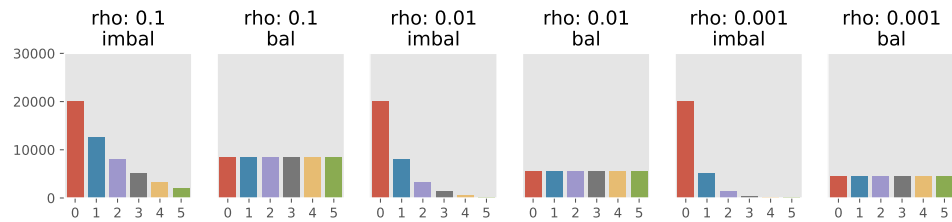


Fig. 5. Visualizing the class distributions for different values of the imbalance ratio  $\rho$ . We always set the more frequent class to 20000 windows whereas the rarest class is set based on the imbalance ratio. The rest of the classes are populated based on the exponential  $20000 \times e^{\beta(c-1)}$ .

*Source dataset imbalance.* As in [43, 74] we first define the imbalance ratio  $\rho$  as the ratio of the rarest class to the most frequent class. Therefore,  $\rho = \frac{\text{num\_windows of the rarest class}}{\text{num\_windows of the most frequent class}} \leq 1$ . We artificially create balanced and imbalanced subsets by using an exponential distribution given by  $20,000 \times e^{\beta(c-1)}$  where 20,000 corresponds to the number of windows of the majority (the most frequent) class,  $e$  is the exponential function,  $c$  is the class index, and  $\beta$  is a scaling factor. For example, if we have an imbalance ratio  $\rho = 0.01$ , the rarest class will have 200 windows, whereas the most frequent class has 20,000 windows, and the remaining classes are populated according to the exponential. Therefore, the total number of windows is dependent on the class imbalance ratio.

We study three class imbalance ratios  $\rho \in \{0.001, 0.01, 0.1\}$  and obtain  $\{\sim 27k, \sim 33k, \sim 51k\}$  training windows. We chose the most frequent class to have 20,000 windows as the resulting total imbalanced subset size is  $\sim 40k$  windows, or 1% of the Capture-24 train set, which was shown to have comparable performance to using the entire train split in Fig. 4. For every  $\rho$ , the balanced subset divides the total number of windows in the imbalanced subset for that  $\rho$  by the number of classes, which is 6. For example, given a  $\rho$  of 0.001, the total number of windows is  $\sim 27k$  in the imbalanced subset, and thus, each class of the balanced subset contains  $\sim 4.5k$  windows. A visualization of this setup is shown in Fig. 5. In practice, we perform five randomized runs for the pre-training and in each case, the most frequent and the rarest classes are chosen randomly, thereby making the aggregated performance resistant the choice of the majority class.

The performance of the self-supervised methods under varying levels of dataset imbalance  $\rho$  is shown for two randomly chosen datasets in Fig. 6 (to study the performance on all target datasets, refer to Fig. 16 and 17 in the Appendix). For Multi-task self-supervision, Masked reconstruction, and CPC, the performance on both imbalanced and balanced data is nearly identical. Autoencoder on the other hand shows increasing reduction in performance as the source subsets get more imbalanced. For Mobiact, the difference between the means of the balanced and imbalanced runs is  $\sim 0.9\%$  when  $\rho=0.1$  (i.e., the rarest class is 10 times smaller than the most frequent class). This increases to  $\sim 2\%$  and  $\sim 3.3\%$  when  $\rho$  is 0.01 and 0.001 respectively. Myogym follows a similar trend, with reduction  $\in \sim\{0.5\%, 1.6\%, 2.4\%\}$  when  $\rho \in \{0.1, 0.01, 0.001\}$ . Thus, the performance gets worse as the pre-training is exposed to increasingly imbalanced subsets. Further, we note that the standard deviation for the Autoencoder also increases considerably with increasing source imbalance. This can be explained by considering the ‘pretext’ task for autoencoders – which involves the reconstruction of input windows. The pre-training is dependent on reconstructing the source data, and limited exposure to windows of the rarest class renders the model unable to reconstruct them accurately, thereby resulting in less effective representation learning. As the rarest class reduces in size with decreasing  $\rho$ , the downstream activity recognition performance also drops slightly (i.e.,  $\sim 3.3\%$  at worst for Mobiact). Fig. 6, 16 and 17 reveal the robustness of the self-supervised approaches to class imbalance in the source dataset. This is a strong point in favor of utilizing self-supervision, as class imbalance in the source dataset does not strongly affect the downstream activity recognition performance. As such, this means that the source dataset need not be artificially balanced for effective performance; rather, the unavailability of even coarse labels (for balancing) is not a crutch for learning useful representations.

*Target dataset imbalance.* Next, we study the class imbalance from the target dataset standpoint. We choose three datasets, one from each on-body position having significant dataset imbalance – Wetlab, Mobiact, and PAMAP2. The native class composition of the datasets and their imbalances is visualized in Fig. 15 in the Appendix. Once again, we utilize the imbalance ratio as defined previously in order to balance the train split of the target datasets, wherein  $\rho$  is ratio of the number of windows of rarest class to the most frequent class. However, in contrast to the source imbalance setup, setting the class sizes based on the exponential is not possible as the minority class sizes are significantly lower than the most frequent class, and often other class sizes are lower than the number of windows dictated by the exponential. Therefore, we limit the maximum size of all classes based on the imbalance ratio  $\rho$  and the size of the smallest class. For example, if  $\rho$  equals 1, then **all** classes have the same number of windows, equalling the rarest class (i.e., the total size of the train split is correspondingly

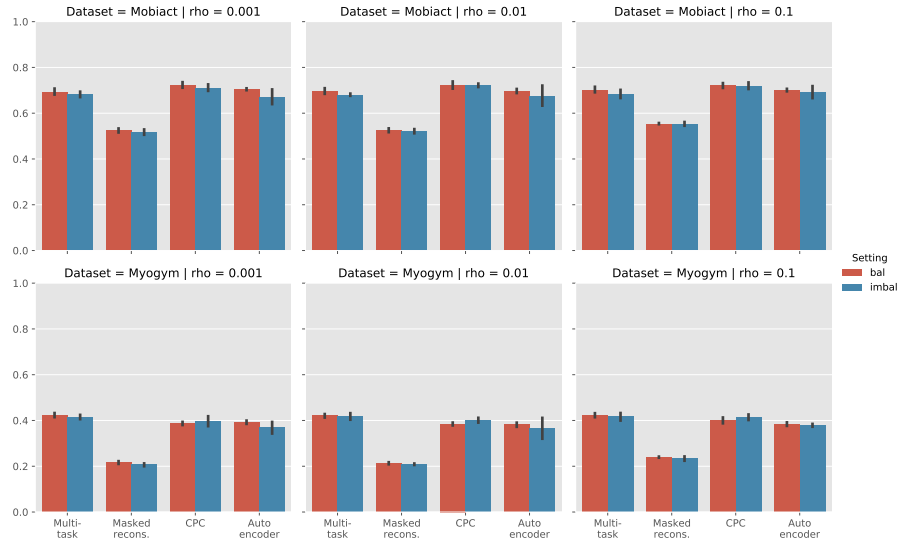


Fig. 6. Studying the effect of imbalance in the source dataset: we artificially create subsets of the source dataset with varying amounts of imbalance, and utilize them for pre-training. The activity recognition is performed per usual with five fold validation on the target datasets, and five randomized runs for both the pre-training and classification. We only show the visualization on two target datasets for clarity. The remaining results are a part of the appendix (Fig. 16 and 17). We note that all self-supervised methods are robust to class imbalances, with only minor differences in performance between balanced and imbalance source subsets.

the smallest). Similarly, if  $\rho = 0.01$ , then the most frequent class is set to have 100x more windows than the rarest class. However, if any class exceeds this number, the windows are randomly sub-sampled to match the maximum allowed size. A visualization of setup is shown in Fig. 18 in the Appendix. The total size of the dataset is dependent on the imbalance ratio  $\rho$ , resulting in for example,  $\{\sim 1.1k, \sim 9.3k, \sim 17.5k, \sim 34.5k, \sim 38.7k\}$  training windows when  $\rho \in \{1, 10, 25, 100, 200\}$  for the train split of the first fold of Mobiact.

We utilize the best performing pre-trained models from Tab. 3 and 4 and train activity recognition models on subsets with varying  $\rho$  of the train split. The validation and test splits are kept untouched and five-fold validation is performed for five randomized runs, and visualized in Fig. 7. As seen in the class composition diagram (Fig. 15), the native imbalance ratio for the train splits of Wetlab, Mobiact, and PAMAP2 are approx.  $\{0.01, 0.008, 0.1\}$  respectively. For Wetlab and Mobiact, we note that the performance under balanced conditions (i.e.,  $\rho = 1$ ) is considerably lower than when there is significant imbalance, such as  $\rho = 0.01$ . As the total size of the training set is dependent on the imbalance ratio and the native imbalance for these datasets is severe, the number of windows available for training are much lower (for example,  $\sim 1.1k$  windows when  $\rho = 1$  for Mobiact, as mentioned above). Thus, the small size of the training dataset has a large impact on the performance, thereby leading to degraded activity recognition. For these datasets, more imbalance leads to much a larger training dataset, and therefore the performance peaks when the imbalance is around 0.01 or 0.04. However, the worsening imbalance, when  $\rho = 0.005$ , results in reduced performance for all self-supervised methods.

PAMAP2 is an inherently more balanced dataset than both Wetlab and Mobiact. Due to this, the performance drop when  $\rho = 1$  is not as drastic, and the performance increases when  $\rho = 0.1$  (which is close to its native imbalance). However, if the imbalance ratio is reduced, exacerbating the difference in the class sizes, we observe a considerable reduction in the activity recognition for all self-supervised methods. Interestingly, DeepConvLSTM also follows a similar trend for all target datasets. Therefore, for target datasets, the class imbalance has less impact

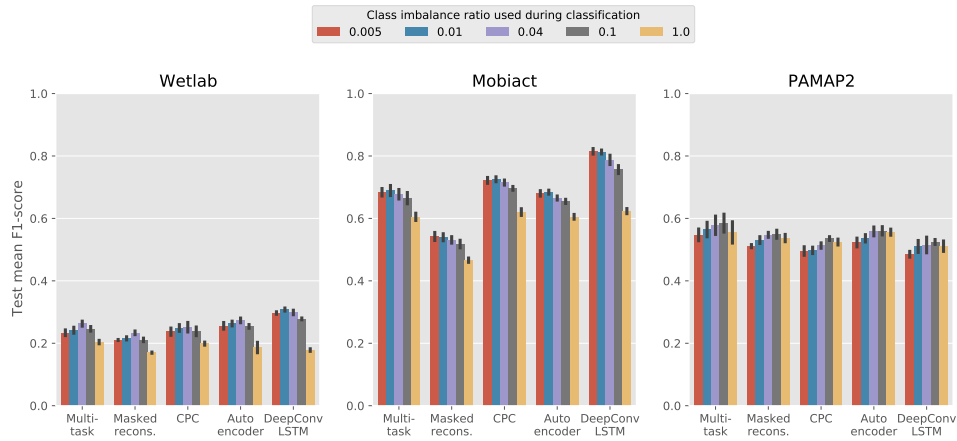


Fig. 7. Studying the effect of self-supervised pre-training on being robust to target dataset class imbalance: we take three imbalanced target datasets – Wetlab, Mobiact, and PAMAP2 – and either make it more balanced by sub-sampling, or make it more imbalanced by removing the minority class. We utilize the best performing models as detailed in Tab. 3 and 4 and perform fine-tuning on the subsets of the train split. We perform five randomized runs including the pre-training and classification for each value of the class imbalance ratio. The mean of the target test set F1-scores are plotted along with the standard deviation for the five runs.

on performance relative to the size of the training set itself, which is encouraging for the use of self-supervised learning methods in HAR.

**5.2.3 Performance under availability of very limited annotated data.** In this criterion, we consider a scenario of vital importance to activity recognition, which is when very limited labeled data are available for classification. This situation can arise when both collecting and annotating data maybe difficult due to cost and privacy concerns, such as in medical applications. Alternatively, real-world deployment may allow for acquiring a small labeled dataset from users without significant interruptions (or during device setup). For such scenarios, it is advantageous to identify methods that can pre-train on a large-scale background dataset, and demonstrate improvements for fine-tuning with limited labels.

We compare the performance of the self-supervised approaches against DeepConvLSTM, which is our supervised baseline. As done previously, we first pre-train with the large-scale Capture-24 dataset and freeze the learned encoder weights. Only the classifier layers are optimized using the available labels. In contrast, the entire DeepConvLSTM network is trained end-to-end with the annotations. We utilize the best performing models from Tab. 3 and 4 for each self-supervised method and DeepConvLSTM. For each target dataset fold, we randomly select  $\{2, 5, 10, 50, 100\}$  labeled windows per class for training whereas the validation and test splits are untouched. We compute the mean of the F1-scores obtained across the five folds, and visualize the performance across five randomized runs in Fig. 8.

First, we observe that the self-supervised approaches generally outperform DeepConvLSTM (shown in yellow in Fig. 8) by a significant margin. For datasets such as Myogym, Wetlab, Daphnet FoG etc., which contain activities that are at least not partially covered in the Capture-24 dataset (see Tab. 4 for reference), we see significant improvements in the test set performance. This is encouraging as the learned representations can generalize to unseen activities and improve performance even when sufficient labeled data is not available.

Analyzing across sensor locations, we notice an interesting trend. For HHAR, Myogym, and Wetlab, which are wrist-based, as well as Daphnet, MHEALTH, and PAMAP2, which are leg-based, the self-supervised methods significantly outperform the supervised baseline. However, in the case of Motionsense (which is waist-based),

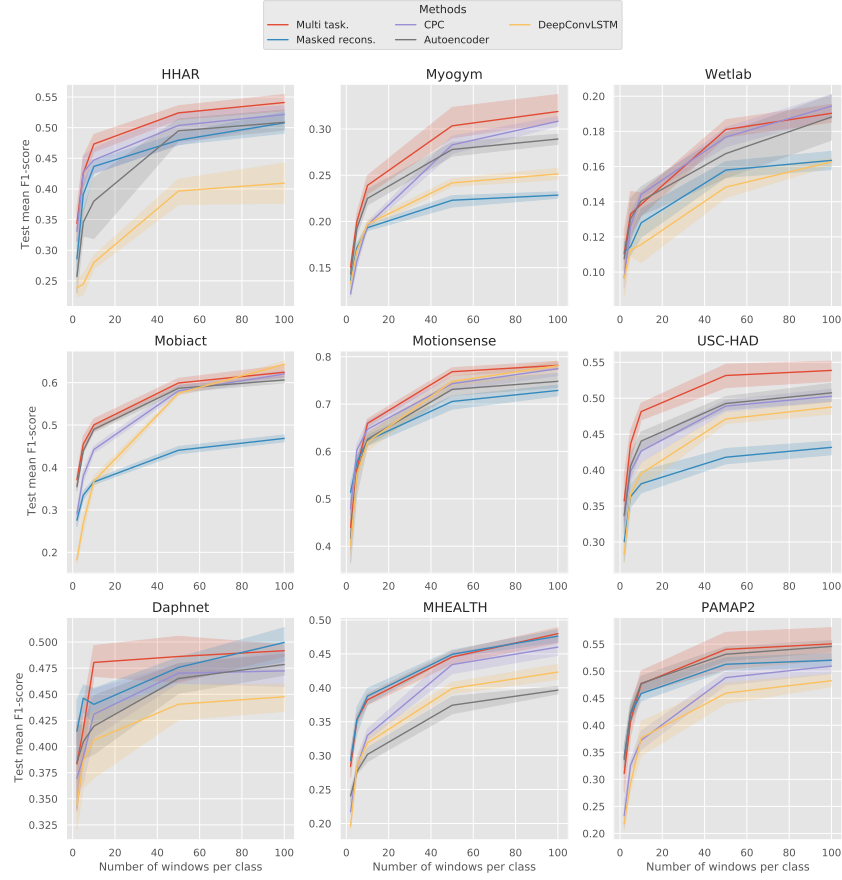


Fig. 8. Studying the performance of the self-supervised methods when there are very limited data available for fine-tuning: we pre-train the self-supervised approaches on Capture-24 and fine-tune them with limited labeled data, where  $\{2, 5, 10, 50, 100\}$  labeled windows per class are available for activity recognition. DeepConvLSTM (in yellow) is trained end-to-end with the available labeled windows. For all methods, the performance across five randomized runs is plotted above. We observe significant improvements over DeepConvLSTM for most target datasets.

DeepConvLSTM performs comparably to self-supervision. Similarly for Mobiact, DeepConvLSTM performs well if there are atleast 50 labeled windows per activity class available. For USC-HAD, Multi-task, CPC, and Autoencoder perform considerably better than end-to-end training. Therefore, self-supervision is more effective when transferring to the wrist-based datasets (which match the source dataset location), or the leg. As discussed in Sec. 5.1.1, this is likely because many activities covered in the leg-based datasets, such as running, walking, going up and down the stairs have synchronized motion between the wrist and legs.

In general, multi-task self-supervision generally shows the highest performance, across sensor positions and target activities. The strong performance of the self-supervised methods, even when such limited annotations are available demonstrates the practical value of the pretrain-then-finetune paradigm, for application in scenarios where only small amount of data maybe collected and annotated.

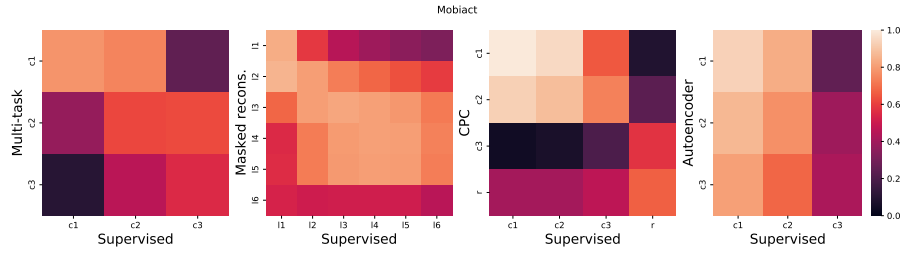


Fig. 9. Studying the representation similarity to supervised learning: we observe higher similarity between early layers trained with self-supervision and supervised learning.

### 5.3 Feature Space Characteristics

In this dimension, we perform an exploration of the feature space itself, in order to understand its properties. This exploration is done across three criteria: first, we compare the similarity of the learned representations to supervised learning, thereby understanding whether the self-supervised approaches capture similar components of the data as in supervised learning, even though they do not have access to target annotations. Subsequently, we gauge the linear separability of the representations, assessing whether the learned features enable all downstream tasks or only specific ones. Finally, we compute the implicit dimensionality of the learned representations for all methods, with the aim of understanding whether the methods fully utilize the representation space or not.

**5.3.1 Similarity to supervised learning.** The gold-standard for activity recognition generally lies in supervised learning, wherein end-to-end training is performed with the available annotations, resulting in the best possible performance. However, the introduction of self-supervised approaches has provided an alternative methodology for learning representations, sometimes even outperforming the supervised counterparts. As such, an interesting investigation is towards understanding if the supervised and self-supervised methods capture similar components of the data, and if so, which layers are most similar. We utilize Linear Centered Kernel Alignment (CKA) [39], which returns a value between 0 and 1 (1: identical), in order to obtain a measure of representation similarity.

For this analysis, we take the first fold of target datasets and perform supervised training with a network identical to the self-supervised architecture. Subsequently, we perform a forward pass on 1,000 randomly chosen windows in order to extract the representations at each convolutional layer (i.e., after the layer itself rather than after dropout and ReLU present in the block) of the networks. Correspondingly, we also extract self-supervised features from previously trained models. We perform a pairwise comparison between representations of self-supervised and supervised methods across five random runs, and visualize the mean for Mobiact in Fig. 9. For clarity, the visualization for all target datasets has been added to the Appendix, in Fig. 19. A similar exploration was also performed in Multi-task self-supervision [58], where Singular Vector Canonical Correlation Analysis (SVCCA) [56] was utilized. CKA is related to SVCCA, yet it is advantageous as it is able to determine correspondence between layers trained with different random initializations, and more importantly, different feature sizes.

From Fig. 9, we observe that the first encoder layer outputs representations that are most similar to supervised learning. As in the original paper for CKA [39], the similarity generally reduces as the depth of the encoder layer increases (see the diagonal of the similarity matrices for reference). This trend is clearer for Masked reconstruction, which contains six Transformer encoder layers. The diagonal elements until layer 5 are very similar, especially in the neighborhood around the diagonal. This indicates that immediately preceding and succeeding layers are more similar than farther layers. For example, layer 1 from the pre-trained Masked reconstruction is more similar to the Supervised layer 2 than layer 6.

In the case of CPC, we observe a sharp drop in the similarity after the second convolutional layer, with the features from third layer being considerably dissimilar to preceding layers. The fourth layer of CPC is the Gated

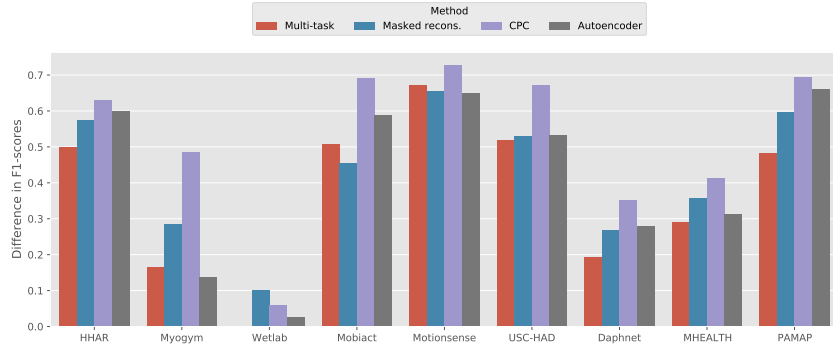


Fig. 10. Studying the linear separability of the learned representations: we compute the difference in the train set F1-score between utilizing ground truth and random labels using a **linear** classifier. We observe that Multi-task self-supervision succeeds more in learning generic representations rather than ones specific to downstream tasks.

Recurrent Unit [9], which also learns representations similar to supervised learning. Finally, the Autoencoder also follows the general trend of higher similarity in the earlier layers with the first two convolutional layers being very similar. Interestingly however, the self-supervised representation from the third layer also shows high similarity to the features from the first supervised layer.

The similarity matrices from Fig. 9 and 19 demonstrate that self-supervised approaches have the capability to learn representations similar to end-to-end training. More specifically, the earlier layers of the self-supervised network produce very similar representations to supervised learning (a trend also observed in [39]). The similarity of the later layers diverges, likely because the supervised representations capture the more activity-specific characteristics of the data, whereas the self-supervised methods optimize different objectives entirely.

**5.3.2 Linear separability of the representations.** One of the aims of the pretrain-then-finetune paradigm is to learn generic representations from a large body of unlabeled movement data, such that *any* downstream task/scenario can leverage the pre-trained weights. This criterion studies whether the self-supervised methods learn representations that are only useful for certain downstream tasks or scenarios, or whether they enable all tasks by creating a representation space wherein many labelings of the data are expressible as linear classifiers [71]. In order to quantify such separability, we utilize the protocol detailed by Wallace *et al.* [71] where linear classifiers are trained on the learned encoder weights, but with random labels. The performance obtained by using the random annotations is contrasted against utilizing the ground truth, and their difference is plotted in Fig. 10. Methods that have a smaller difference in the linear classification performance between using ground truth and random labels learn generic feature descriptors rather than capturing representations that are only relevant to some downstream scenarios [71]. In Fig. 10, we perform five randomized runs for both the pre-training and the linear classification, and plot the difference in the mean of the train set F1-scores.

We observe that Multi-task self-supervision generally has a lower difference in the performance between ground truth and randomized labels, indicating that it learns more general representations that enable various downstream scenarios. This is less true for the other methods, with CPC learning the least generic features.

**5.3.3 Implicit dimensionality of the representations.** The dimensionality of the features used for activity recognition is of importance from a wearables standpoint, as lower feature dimensions result in reduced computational costs and computational time during classification [29]. Approaches that can perform effectively while also resulting in smaller features are more desirable due to the computational savings they offer. At the same time, larger representation sizes can benefit from the availability of more training data [38]. As detailed in [71], we study the implicit dimensionality of the learned representations through Principal Component Analysis. The

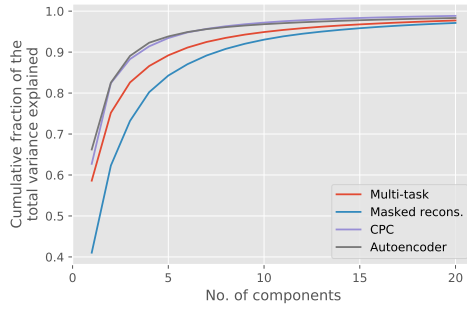


Fig. 11. Studying the implicit dimensionality of the learned representations: the cumulative fraction of the total variance across the first twenty principal components is averaged across all datasets and visualized. We observe that Masked reconstruction has the lowest explained variance thereby indicating *higher* implicit dimensionality.

goal of this analysis is to quantify the percentage of the total variance explained by the first  $n = 20$  principal components. Higher percentage of the total variance being explained by the first 20 components (or fewer) indicates relatively *lower* implicit dimensionality.

As in Sec. 5.3.2, we perform inference using the best performing pre-trained models from Tab. 3 and 4 on the first fold of the target datasets. We randomly sample 1,000 training windows in five randomized runs and extract the representations from the last encoder layer. In order to make the feature sizes comparable, we utilize the last convolutional layer from CPC for extraction rather than the GRU. Principal Component Analysis (PCA) is performed on the extracted features for each target dataset, and the cumulative fraction of the explained variance is averaged across the five randomized runs. Following [71], the cumulative fraction of total variance explained in Fig. 11 is obtained by once again computing the mean across all target datasets. For reference, the implicit dimensionality of the learned representations has been visualized individually for each target dataset in Fig. 20 in the Appendix.

In Fig. 11, we see that for both CPC and Autoencoder, around 95% of the variance can be explained from the first five components itself, which increases to over 98% when considering 20 components. In contrast, for Multi-task self-supervision, less than 90% of the variance can be explained using five components. It is lower still for Masked reconstruction, at around 85%. As most of the variance can be explained for CPC and Autoencoder using just five components, they have relatively lower implicit dimension. On the other hand, Multi-task self-supervision and Masked reconstruction utilize the latent space more effectively and have higher implicit dimensionality.

## 6 DISCUSSION

The main goal of this work is to deepen our understanding of self-supervised approaches for human activity recognition using wearables. We accomplish this by conducting a large-scale study utilizing the assessment framework, which comprises of a *collection* of criteria. The first part of this section investigates two choices in our experimental setup – first, that it is advantageous to utilize the source dataset normalization statistics for target dataset normalization; and, second, simple encoder architectures may not be sufficient for effective representation learning. The latter part contains a retrospective of the empirical study, wherein we present the benefits and downsides of each self-supervised technique, and summarize the insights gained. Lastly, we also discuss desirable characteristics for such assessment frameworks, and chart a research agenda for future versions.

### 6.1 Applying Source Dataset Normalization to Target Scenario for Activity Recognition

For all experiments conducted in our study, the pre-processing for the target datasets included applying the normalization means and variances from the source (Capture-24) training set so as to bring the dataset statistics

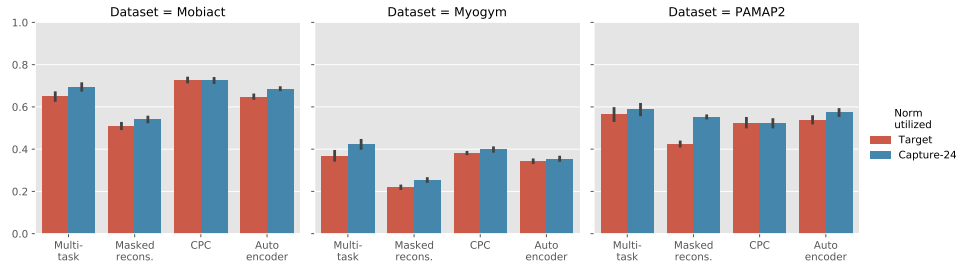


Fig. 12. Studying whether the source dataset means and variances must be utilized for pre-processing the target datasets during activity recognition: we plot the activity recognition performance when the target datasets are normalized based on the source dataset statistics, or the target data itself. There is a significant improvement in performance obtained by utilizing the source dataset (Capture-24) means and variances. For clarity, we only show the performance on one dataset per sensor location in this figure. The rest are contained in Fig. 21 in the Appendix.

closer. This practice of applying normalization using the source dataset means and variances is utilized for transfer learning [32]. In this section, we study and quantify whether the source dataset means and variances must be applied at all for wearables-based self-supervised transfer learning.

We repeat the setup for activity recognition from Tab. 3 and 4 while either performing normalization based on the source dataset statistics or based on the target dataset itself. The test-set F1-score obtained after five-fold validation and five randomized runs is visualized in Fig. 12. For clarity, we choose one dataset from each sensor location and present the results in the aforementioned figure.

In general, the utilization of the source normalization statistics results in clear improvements over normalizing based on the target data itself. In the case of Mobiact, Multi-task self-supervision, Masked reconstruction and Autoencoder show a considerable increase in performance when the Capture-24 normalization statistics are utilized. This trend is observed for PAMAP2 as well with Masked reconstruction and the Autoencoder demonstrating substantial improvements. For Myogym, Multi-task self-supervision shows the largest difference in performance with the usage of source dataset statistics. Overall, we note that utilizing the Capture-24 training dataset normalization parameters has the highest impact on Masked Reconstruction and Autoencoder. This makes sense as the ‘pretext’ for these methods involves reconstructing the input windows (or masked portions of it), and thus applying normalization using the source dataset mean and variances results in similar data statistics. Therefore, it is clearly advantageous to utilize the source dataset normalization’s means and variances during self-supervised transfer learning.

## 6.2 Is the Performance of Self-Supervision Getting Hampered by (Too) Simple Encoder Architectures?

In our study of the quantity of the unlabeled source dataset windows required for pre-training (see Fig. 4), we observed that using only 10% of the training windows results in comparable if not better downstream activity recognition. We hypothesized that this was likely due to the simple and shallow encoder architectures employed by these approaches, which comprise generally of three 1D convolutional blocks. Here, we increase the depth of the encoder by adding a larger convolutional block to the encoders, and study the impact on activity recognition. For Multi-task self-supervision, we add a fourth convolutional block containing 128 filters and a kernel size of 4, whereas for CPC, the additional convolutional block comprises of 256 filters with the kernel size of 3, matching the previous layers. Similarly for the Autoencoder, the new convolutional block contains 256 filters and a kernel size of 9. We do not perform this analysis for Masked reconstruction as the best overall model during pre-training contains six Transformer [69] encoder layers and is thus a large encoder.

The pre-training is performed for increasing quantities of randomly sampled pre-training windows, similar to the analysis in Fig. 4, across five randomized runs of sampling the source windows and pre-training, to the

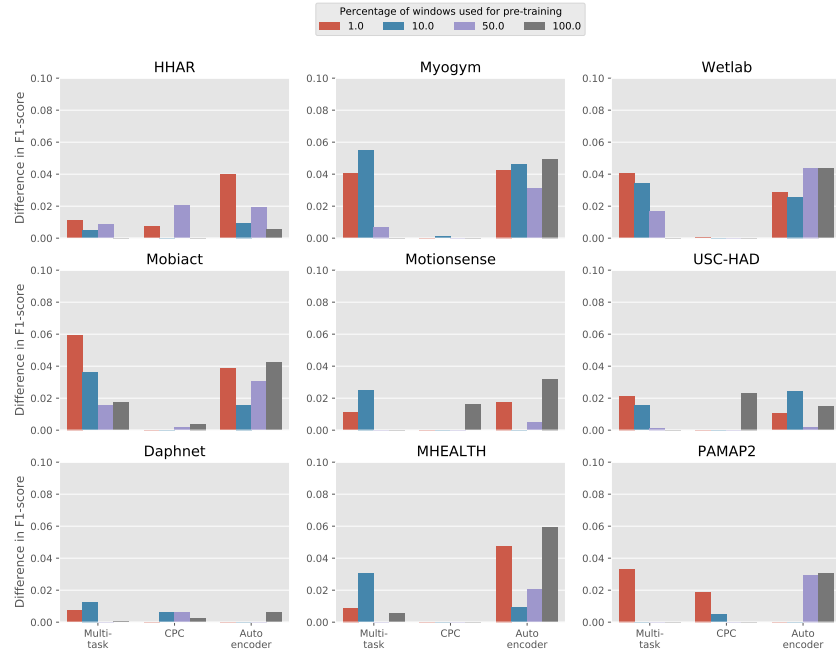


Fig. 13. Studying the impact of deeper encoder architectures: we increase the depth of the encoder for Multi-task self-supervision, CPC, and Autoencoder by adding an additional convolutional block. We plot the difference in the mean of the test set mean F1-scores across five folds of the original and deeper encoder architectures for increasing quantities of pre-training windows. Note that a positive difference indicates worsening performance with additional layers. CPC shows no change with the addition of another convolutional block in its encoder.

five fold validation and activity recognition. The difference in the mean of the five-fold F1-score for the original encoder architecture and the deeper variant are plotted for all target datasets in Fig. 13. In the figure, increasing differences indicate reduced performance resulting from the addition of an extra layer.

We note that there is very limited difference in F1-scores for CPC, for increasing quantities of the source data, indicating that the additional convolutional block did not have any discernable effect on performance. For both Multi-task self-supervision and Autoencoder, the performance reduces with the addition of another encoder layer, indicating that such naive increase in encoder depth does not show a corresponding improvement in activity recognition, even if more pre-training data are available. Another likely reason for the reduction in performance is that this experiment utilizes the best overall parameters as determined in Tab. 3 and 4. It is possible that these hyperparameter settings are not ideal for the increased depth of the encoder.

### 6.3 Advantages and Drawbacks of Self-Supervised Approaches

We have performed a large scale empirical study into assessing the state of the *pretrain-then-finetune* paradigm that is gaining widespread adoption by the wearables community. In such a paradigm, a large-scale background movement dataset can be utilized to learn effective representations with the goal of enabling a host of diverse downstream scenarios, some of which may have difficulty in collecting data or obtaining annotations. Here, we summarize the benefits and drawbacks of each of the evaluated methods from different standpoints as encountered during the course of this study – such as the training time, computational load, and complexity of the approach, and tabulate them into Tab. 5.

Table 5. A brief summary of the advantages and drawbacks of each self-supervised method. ~ indicates that the implementation is neither simple nor too complex.

Approach	Simple encoder	Quick training	Low computational load	Simple Implementation	Small hyperparameter space
Multi-task	✓	✗	✓	~	✓
Masked recons.	✗	✗	✗	~	✓
CPC	✓	✗	✗	✗	✗
Autoencoder	✓	✓	✓	✓	✓

Multi-task self-supervision [58] jumpstarted the investigation into the applicability of self-supervision for human activity recognition. The main advantage of utilizing this approach lies in its effectiveness in learning representations that are applicable for a variety of downstream scenarios, as evidenced by its overall superior performance in Tab. 3 and 4. The transformation techniques applied in this method are well designed for learning representations for accelerometer data. The encoder architecture is simple, resulting in small GPU memory footprint during pre-training as well as fine-tuning. The hyperparameter space we utilized is also small, consisting primarily of the learning rate and L2 regularization. However, there is a host of hyperparameters regarding the signal transformations which can be tuned for improved performance (we do not perform that exploration in this study). One drawback includes its relatively poor performance on multi-sensor datasets [30, 31] as the data transformations are specifically designed for accelerometry and cannot be trivially applied to other sensors, for example, gyroscopes and magnetometers, which are typically part of the IMU setups.

Autoencoders are one of the most well established unsupervised learning approaches. The primary benefit of utilizing autoencoders lies in their simplicity, with the encoder and decoder architectures being mirror images of each other, and the objective corresponding to simply reconstructing the original signal. Therefore, they are easy to setup and typically one of the baselines against which self-supervised methods are compared. Additionally, we observe in our study that Autoencoders often perform comparably to more sophisticated methods such as Multi-task self-supervision or CPC. Given the simplicity of the architecture and the objective, the training time is also significantly shorter relative to other methods, while also being less stressful from a computational perspective. The hyperparameter space is small as well, covering the learning rate, L2 regularization and the convolutional kernel size. The disadvantage of utilizing autoencoders is that it may not result the best possible unsupervised performance. Additionally, care must be taken to not learn an identity function, thereby resulting in less useful representations.

Contrastive Predictive Coding (CPC) [31] learns representations by predicting multiple future timesteps of sensory data and optimizing via the InfoNCE [67] loss. The encoder architecture is simple, and the approach generally performs well across target scenarios. A strength of this method lies in its applicability and superior performance on multi-sensor data [31], and in scenarios where transition-style activities are present (for example, getting in and out of a car, as in Mobiact). A downside to this approach is that it requires considerable parameter tuning, including learning rate and weight decay, future prediction horizon, and batch size. Additionally, care must be taken for encoder design and sampling negatives to not produce trivial pre-training, resulting in useless representations. The training time is considerable, and extends particularly with increasing prediction horizons.

Lastly, Masked reconstruction [30] is trained by reconstructing only masked out timesteps of the window. Therefore, a strong point in favor of this approach is that the architecture setup and the training objective are straightforward. However, as seen in this study, the approach does not generally perform comparably to other self-supervised approaches for learning representations on a single accelerometer. Additionally, the Transformer [69] encoder architecture is large and computationally intensive, and has the longest training time by far in this study. The hyperparameter space contains a few parameters, including the number of warmup steps in the

learning schedule, the number of Transformer encoder layers and heads, and the percentage of time-steps to be masked. In the original paper [30] however, this method outperforms supervised and unsupervised baselines on two out of four benchmark datasets which contain data from both an accelerometer and a gyroscope.

Overall, the aim of discussing the pros and cons of each approach is to bring to light other viewpoints regarding these methods that may not immediately be obvious by only considering the resulting activity recognition performance. Doing so empowers practitioners in the community in making more informed judgement for applying these methods to diverse target scenarios.

#### 6.4 The Necessity for an Evolving Benchmark and a Call to Action

Over the last few years, the human activity recognition community has seen a growing interest into studying and developing self-supervised representation learning methods. These approaches strike at the heart of the small labeled dataset problem prevalent in sensor datasets, and therefore present the ‘pretrain-then-finetune’ paradigm shift. In moving away from designing end-to-end architectures that rely solely on the availability of annotated datasets, these methods exploit potentially large-scale unlabeled data to pre-train generic representations that can be subsequently fine-tuned to the specific activities of interest, positively impacting scenarios where data collection and annotation are beset with cost and privacy challenges. Techniques towards understanding their performance has so far been limited to one view – wherein the source and target conditions such as sensor locations and activities are similar.

In this work, we follow the philosophy espoused by natural language processing benchmarks such as GLUE [72] and GEM [19], which argues that evaluation on a *suite* of tasks is necessary for a well-rounded understanding of model performance. More specifically, our assessment is similar to GEM, wherein the goal is to foster a nuanced analysis and discussion of performance by the community, unencumbered by relentless pursuit of hill climbing and leaderboards. As such, this work presents the *v1.0* into evaluating the current state-of-the-field.

With the evolution of the field and introduction of increasingly effective and complex techniques, the evaluation and benchmarks need to be updated in tandem with contributions from the community. The solved tasks need to be replaced with more challenging and relevant ones, addressing discovered flaws in the established experimental setups [19]. Therefore, this work presents a call-to-action for the wearables community as a whole so that we can collectively update and evolve the assessment framework alongside the progress of the field, so that future versions of the framework are large-scale, decentralized community efforts.

#### 6.5 Lessons Learned and Insights Gained

Through the course of conducting this large-scale empirical study, we have discovered several insights and learned lessons into the behavior of self-supervised methods under diverse conditions. Here, we summarize them with brevity for easy reference:

- (1) Self-supervised methods are effective in scenarios where target sensor location does not match the source location, with transfer from the wrist→leg being more successful than wrist→waist.
- (2) The approaches have the capability to generalize well to potentially unseen activity classes during downstream recognition, including fine-grained gym exercises such as curls and rows, and medical applications involving recognizing the freeze of gait symptoms in Parkinson’s disease.
- (3) The target dataset sampling rate must match the source conditions for optimal performance.
- (4) The techniques are data efficient and perform comparably while only utilizing a small fraction of the available data – both from a participant as well as quantity of data standpoints – thereby reducing the computational burden. By and large, a small yet diverse dataset (in terms of participants) can result in better recognition than collecting lots of data from a few participants.

- (5) Self-supervised learning is surprisingly robust to even extreme imbalances in the source dataset whereas the target dataset imbalance has limited impact on performance.
- (6) These approaches have strong practical value, exhibiting significant improvements in scenarios where labeled data is at a premium.
- (7) Early layers of the learned encoders show high similarity to supervised learning, whereas the features diverge deeper into the network. Also, layers closer to each other are more similar than those farther apart.
- (8) Multi-task self-supervision succeeds in learning the most generic features of wearable data, and thereby enables wide variety of downstream tasks.
- (9) Masked reconstruction has the highest implicit dimensionality and thus more efficiently makes use of the learned representation space.
- (10) Utilizing the means and variances of the source dataset normalization on the target dataset results in considerable performance gains.

## 7 SUMMARY AND CONCLUSION

The field of human activity recognition using wearables (HAR) is currently undergoing a transition regarding the de-facto standard for how to model and recognize activities. The community has begun to move away from designing complex end-to-end architectures that require large quantities of annotated data, and rather focuses on leveraging—easier to collect—unlabeled sensor data to derive generic data representations that are then subsequently fine-tuned to the specific downstream scenarios. Recently, especially self-supervised approaches have demonstrated great promise towards more robust modeling and thus improved activity recognition performance but also opened up new HAR application domains.

In this work, we aimed at assessing the state-of-the-field of self-supervision in HAR research. We conducted a systematic, large-scale "stress test" of these contemporary methods under a variety of conditions. We formulated and introduced an assessment framework that comprises of three dimensions, each containing three criteria, which collectively shed light on different aspects of the models. The first dimension studies the robustness of these approaches when the source and target conditions are not similar, whereas the impact of the dataset characteristics such as class imbalance and quantity of data available is investigated in the second dimension. The third dimension explores the learned representation space, probing the linear separability, implicit dimensionality, and similarity to supervised learning. Put together, these dimensions allow for a multi-faceted evaluation of the model performance, and an inventory of the state of self-supervised human activity recognition research.

Using this assessment framework, we performed our evaluation study on a curated collection of nine benchmark datasets, which are diverse in terms of the sensor locations, activities under study, data size, and the number of participants. The study revealed a collection of insights regarding model behavior, for example, the robustness of self-supervised methods towards class imbalances, and the ability to produce significant improvements over supervised learning when there is a scarcity of annotations. These results and findings are encouraging as they indicate the broad applicability of these self-supervised methods in wide-ranging target scenarios, and affirm the capability of these techniques for empowering human activity recognition in applications where data both collection and annotation may be challenging to accomplish.

Our assessment framework should be considered as *v1.0* that allowed us develop a deeper understanding of self-supervised learning methods in the field of wearables-based human activity recognition (HAR). We call upon the research community for action to collectively contribute towards evolving this framework and using it as a standard for model development and evaluation in our field. We aim at releasing the framework in an accessible form that will allow researchers and practitioners to employ it for their model development and deployment activities, which—overall—will allow the community to push the state-of-the-art in HAR.

## REFERENCES

- [1] Yuki M Asano, Christian Rupprecht, and Andrea Vedaldi. 2019. A critical analysis of self-supervision, or what we can learn from a single image. *arXiv preprint arXiv:1904.13132* (2019).
- [2] Marc Bachlin, Meir Plotnik, Daniel Roggen, Inbal Maidan, Jeffrey M Hausdorff, Nir Giladi, and Gerhard Troster. 2009. Wearable assistant for Parkinson’s disease patients with the freezing of gait symptom. *IEEE Transactions on Information Technology in Biomedicine* 14, 2 (2009), 436–446.
- [3] Oresti Banos, Rafael Garcia, Juan A Holgado-Terriza, Miguel Damas, Hector Pomares, Ignacio Rojas, Alejandro Saez, and Claudia Villalonga. 2014. mHealthDroid: a novel framework for agile development of mobile health applications. In *International workshop on ambient assisted living*. Springer, 91–98.
- [4] Dominika Basaj, Witold Oleszkiewicz, Igor Sieradzki, Michał Górszczak, Barbara Rychalska, Tomasz Trzciński, and Bartosz Zieliński. 2021. Explaining self-supervised image representations with visual probing. Freiburg, Germany: International Joint Conferences on Artificial Intelligence.
- [5] James Bergstra and Yoshua Bengio. 2012. Random search for hyper-parameter optimization. *Journal of machine learning research* 13, 2 (2012).
- [6] Mathilde Caron, Hugo Touvron, Ishan Misra, Hervé Jégou, Julien Mairal, Piotr Bojanowski, and Armand Joulin. 2021. Emerging properties in self-supervised vision transformers. In *Proceedings of the IEEE/CVF International Conference on Computer Vision*. 9650–9660.
- [7] S Chan Chang and A Doherty. 2021. Capture-24: Activity tracker dataset for human activity recognition. (2021).
- [8] Charikleia Chatzaki, Matthew Pediaditis, George Vavoulas, and Manolis Tsiknakis. 2016. Human daily activity and fall recognition using a smartphone’s acceleration sensor. In *International Conference on Information and Communication Technologies for Ageing Well and e-Health*. Springer, 100–118.
- [9] Junyoung Chung, Caglar Gulcehre, KyungHyun Cho, and Yoshua Bengio. 2014. Empirical evaluation of gated recurrent neural networks on sequence modeling. *arXiv preprint arXiv:1412.3555* (2014).
- [10] Yu-An Chung, Yonatan Belinkov, and James Glass. 2021. Similarity analysis of self-supervised speech representations. In *ICASSP 2021-2021 IEEE International Conference on Acoustics, Speech and Signal Processing (ICASSP)*. IEEE, 3040–3044.
- [11] Yu-An Chung and James Glass. 2020. Generative pre-training for speech with autoregressive predictive coding. In *ICASSP 2020-2020 IEEE International Conference on Acoustics, Speech and Signal Processing (ICASSP)*. IEEE, 3497–3501.
- [12] Yu-An Chung and James Glass. 2020. Improved speech representations with multi-target autoregressive predictive coding. *arXiv preprint arXiv:2004.05274* (2020).
- [13] Yu-An Chung, Wei-Ning Hsu, Hao Tang, and James Glass. 2019. An unsupervised autoregressive model for speech representation learning. *arXiv preprint arXiv:1904.03240* (2019).
- [14] Elijah Cole, Xuan Yang, Kimberly Wilber, Oisin Mac Aodha, and Serge Belongie. 2021. When does contrastive visual representation learning work? *arXiv preprint arXiv:2105.05837* (2021).
- [15] Alexis Conneau, German Kruszewski, Guillaume Lample, Loïc Barrault, and Marco Baroni. 2018. What you can cram into a single vector: Probing sentence embeddings for linguistic properties. *arXiv preprint arXiv:1805.01070* (2018).
- [16] Jacob Devlin, Ming-Wei Chang, Kenton Lee, and Kristina Toutanova. 2018. Bert: Pre-training of deep bidirectional transformers for language understanding. *arXiv preprint arXiv:1810.04805* (2018).
- [17] Aiden Doherty, Dan Jackson, Nils Hammerla, Thomas Plötz, Patrick Olivier, Malcolm H Granat, Tom White, Vincent T Van Hees, Michael I Trenell, Christopher G Owen, et al. 2017. Large scale population assessment of physical activity using wrist worn accelerometers: the UK biobank study. *PLoS one* 12, 2 (2017), e0169649.
- [18] Max Eichler, Gözde Gülgahin, and Iryna Gurevych. 2019. LINSPECTOR WEB: A multilingual probing suite for word representations. *arXiv preprint arXiv:1907.11438* (2019).
- [19] Sebastian Gehrmann, Tosin Adewumi, Karmanya Aggarwal, Pawan Sasanka Ammanamanchi, Aremu Anuoluwapo, Antoine Bosselut, Khyathi Raghavi Chandu, Miruna Clinciu, Dipanjan Das, Kaustubh D Dhole, et al. 2021. The gem benchmark: Natural language generation, its evaluation and metrics. *arXiv preprint arXiv:2102.01672* (2021).
- [20] Robert Geirhos, Kantharaju Narayananappa, Benjamin Mitzkus, Matthias Bethge, Felix A Wichmann, and Wieland Brendel. 2020. On the surprising similarities between supervised and self-supervised models. *arXiv preprint arXiv:2010.08377* (2020).
- [21] Jonathan Gershuny, Teresa Harms, Aiden Doherty, Emma Thomas, Karen Milton, Paul Kelly, and Charlie Foster. 2020. Testing self-report time-use diaries against objective instruments in real time. *Sociological Methodology* 50, 1 (2020), 318–349.
- [22] Spyros Gidaris, Praveer Singh, and Nikos Komodakis. 2018. Unsupervised representation learning by predicting image rotations. *arXiv preprint arXiv:1803.07728* (2018).
- [23] Sixue Gong, Vishnu Naresh Boddeti, and Anil K Jain. 2019. On the intrinsic dimensionality of image representations. In *Proceedings of the IEEE/CVF Conference on Computer Vision and Pattern Recognition*. 3987–3996.
- [24] Priya Goyal, Dhruv Mahajan, Abhinav Gupta, and Ishan Misra. 2019. Scaling and benchmarking self-supervised visual representation learning. In *Proceedings of the ieee/cvf International Conference on computer vision*. 6391–6400.

- [25] Tom George Grigg, Dan Busbridge, Jason Ramapuram, and Russ Webb. 2021. Do Self-Supervised and Supervised Methods Learn Similar Visual Representations? *arXiv preprint arXiv:2110.00528* (2021).
- [26] Nils Hammerla and Thomas Ploetz. 2015. Let's (not) Stick Together: Pairwise Similarity Biases Cross-Validation in Activity Recognition. In *Proc. UbiComp*.
- [27] Nils Yannick Hammerla, James Fisher, Peter Andras, Lynn Rochester, Richard Walker, and Thomas Plötz. 2015. PD disease state assessment in naturalistic environments using deep learning. In *Twenty-Ninth AAAI conference on artificial intelligence*.
- [28] Nils Y Hammerla, Reuben Kirkham, Peter Andras, and Thomas Ploetz. 2013. On preserving statistical characteristics of accelerometry data using their empirical cumulative distribution. In *Proceedings of the 2013 international symposium on wearable computers*. 65–68.
- [29] Harish Haresamudram, David V Anderson, and Thomas Plötz. 2019. On the role of features in human activity recognition. In *Proceedings of the 23rd International Symposium on Wearable Computers*. 78–88.
- [30] Harish Haresamudram, Apoorva Beedu, Varun Agrawal, Patrick L Grady, Irfan Essa, Judy Hoffman, and Thomas Plötz. 2020. Masked reconstruction based self-supervision for human activity recognition. In *Proceedings of the 2020 International Symposium on Wearable Computers*. 45–49.
- [31] Harish Haresamudram, Irfan Essa, and Thomas Plötz. 2021. Contrastive predictive coding for human activity recognition. *Proceedings of the ACM on Interactive, Mobile, Wearable and Ubiquitous Technologies* 5, 2 (2021), 1–26.
- [32] Tong He, Zhi Zhang, Hang Zhang, Zhongyue Zhang, Junyuan Xie, and Mu Li. 2019. Bag of tricks for image classification with convolutional neural networks. In *Proceedings of the IEEE/CVF Conference on Computer Vision and Pattern Recognition*. 558–567.
- [33] Geoffrey Hinton, Oriol Vinyals, Jeff Dean, et al. 2015. Distilling the knowledge in a neural network. *arXiv preprint arXiv:1503.02531* 2, 7 (2015).
- [34] Shruthi K Hiremath and Thomas Plötz. 2020. Deriving effective human activity recognition systems through objective task complexity assessment. *Proceedings of the ACM on Interactive, Mobile, Wearable and Ubiquitous Technologies* 4, 4 (2020), 1–24.
- [35] Tâm Huynh and Bernt Schiele. 2005. Analyzing features for activity recognition. In *Proceedings of the 2005 joint conference on Smart objects and ambient intelligence: innovative context-aware services: usages and technologies*. 159–163.
- [36] Sergey Ioffe and Christian Szegedy. 2015. Batch normalization: Accelerating deep network training by reducing internal covariate shift. In *International conference on machine learning*. PMLR, 448–456.
- [37] Aftab Khan, Nils Hammerla, Sebastian Mellor, and Thomas Plötz. 2016. Optimising sampling rates for accelerometer-based human activity recognition. *Pattern Recognition Letters* 73 (2016), 33–40.
- [38] Alexander Kolesnikov, Xiaohua Zhai, and Lucas Beyer. 2019. Revisiting self-supervised visual representation learning. In *Proceedings of the IEEE/CVF conference on computer vision and pattern recognition*. 1920–1929.
- [39] Simon Kornblith, Mohammad Norouzi, Honglak Lee, and Geoffrey Hinton. 2019. Similarity of neural network representations revisited. In *International Conference on Machine Learning*. PMLR, 3519–3529.
- [40] Heli Koskimäki, Pekka Siirtola, and Juha Röning. 2017. Myogym: introducing an open gym data set for activity recognition collected using myo armband. In *Proceedings of the 2017 ACM International Joint Conference on Pervasive and Ubiquitous Computing and Proceedings of the 2017 ACM International Symposium on Wearable Computers*. 537–546.
- [41] Hyeokhyen Kwon, Catherine Tong, Harish Haresamudram, Yan Gao, Gregory D Abowd, Nicholas D Lane, and Thomas Ploetz. 2020. IMUTube: Automatic extraction of virtual on-body accelerometry from video for human activity recognition. *Proceedings of the ACM on Interactive, Mobile, Wearable and Ubiquitous Technologies* 4, 3 (2020), 1–29.
- [42] Yann LeCun, Yoshua Bengio, and Geoffrey Hinton. 2015. Deep learning. *nature* 521, 7553 (2015), 436–444.
- [43] Hong Liu, Jeff Z HaoChen, Adrien Gaidon, and Tengyu Ma. 2021. Self-supervised Learning is More Robust to Dataset Imbalance. *arXiv preprint arXiv:2110.05025* (2021).
- [44] Luca A Lotta, Laura BL Wittmann, Verena Zuber, Isobel D Stewart, Stephen J Sharp, Jian'an Luan, Felix R Day, Chen Li, Nicholas Bowker, Lina Cai, et al. 2018. Association of genetic variants related to gluteofemoral vs abdominal fat distribution with type 2 diabetes, coronary disease, and cardiovascular risk factors. *Jama* 320, 24 (2018), 2553–2563.
- [45] Mohammad Malekzadeh, Richard G Clegg, Andrea Cavallaro, and Hamed Haddadi. 2018. Protecting sensory data against sensitive inferences. In *Proceedings of the 1st Workshop on Privacy by Design in Distributed Systems*. 1–6.
- [46] Vinod Nair and Geoffrey E Hinton. 2010. Rectified linear units improve restricted boltzmann machines. In *Icm*.
- [47] Francisco Javier Ordóñez and Daniel Roggen. 2016. Deep convolutional and lstm recurrent neural networks for multimodal wearable activity recognition. *Sensors* 16, 1 (2016), 115.
- [48] Laura O'Connor, Soren Brage, Simon J Griffin, Nicholas J Wareham, and Nita G Forouhi. 2015. The cross-sectional association between snacking behaviour and measures of adiposity: the Fenland Study, UK. *British journal of nutrition* 114, 8 (2015), 1286–1293.
- [49] Adam Paszke, Sam Gross, Francisco Massa, Adam Lerer, James Bradbury, Gregory Chanan, Trevor Killeen, Zeming Lin, Natalia Gimelshein, Luca Antiga, et al. 2019. Pytorch: An imperative style, high-performance deep learning library. *Advances in neural information processing systems* 32 (2019), 8026–8037.
- [50] Thomas Plötz. 2021. Applying machine learning for sensor data analysis in interactive systems: Common pitfalls of pragmatic use and ways to avoid them. *ACM Computing Surveys (CSUR)* 54, 6 (2021), 1–25.

- [51] Thomas Plötz and Yu Guan. 2018. Deep learning for human activity recognition in mobile computing. *Computer* 51, 5 (2018), 50–59.
- [52] Thomas Plötz, Nils Y Hammerla, and Patrick L Olivier. 2011. Feature learning for activity recognition in ubiquitous computing. In *Twenty-second international joint conference on artificial intelligence*.
- [53] David MW Powers. 2020. Evaluation: from precision, recall and F-measure to ROC, informedness, markedness and correlation. *arXiv preprint arXiv:2010.16061* (2020).
- [54] Alec Radford, Karthik Narasimhan, Tim Salimans, and Ilya Sutskever. 2018. Improving language understanding by generative pre-training. (2018).
- [55] Alec Radford, Jeffrey Wu, Rewon Child, David Luan, Dario Amodei, Ilya Sutskever, et al. 2019. Language models are unsupervised multitask learners. *OpenAI blog* 1, 8 (2019), 9.
- [56] Maithra Raghu, Justin Gilmer, Jason Yosinski, and Jascha Sohl-Dickstein. 2017. Svcca: Singular vector canonical correlation analysis for deep learning dynamics and interpretability. *Advances in neural information processing systems* 30 (2017).
- [57] Attila Reiss and Didier Stricker. 2012. Introducing a new benchmarked dataset for activity monitoring. In *2012 16th international symposium on wearable computers*. IEEE, 108–109.
- [58] Aaqib Saeed, Tanir Ozcelebi, and Johan Lukkien. 2019. Multi-task self-supervised learning for human activity detection. *Proceedings of the ACM on Interactive, Mobile, Wearable and Ubiquitous Technologies* 3, 2 (2019), 1–30.
- [59] Aaqib Saeed, Flora D Salim, Tanir Ozcelebi, and Johan Lukkien. 2020. Federated Self-Supervised Learning of Multisensor Representations for Embedded Intelligence. *IEEE Internet of Things Journal* 8, 2 (2020), 1030–1040.
- [60] Aaqib Saeed, Victor Ungureanu, and Beat Gfeller. 2021. Sense and Learn: Self-supervision for omnipresent sensors. *Machine Learning with Applications* (2021), 100152.
- [61] Philipp M Scholl, Matthias Wille, and Kristof Van Laerhoven. 2015. Wearables in the wet lab: a laboratory system for capturing and guiding experiments. In *Proceedings of the 2015 ACM International Joint Conference on Pervasive and Ubiquitous Computing*. 589–599.
- [62] Karen Simonyan, Andrea Vedaldi, and Andrew Zisserman. 2013. Deep inside convolutional networks: Visualising image classification models and saliency maps. *arXiv preprint arXiv:1312.6034* (2013).
- [63] Nitish Srivastava, Geoffrey Hinton, Alex Krizhevsky, Ilya Sutskever, and Ruslan Salakhutdinov. 2014. Dropout: a simple way to prevent neural networks from overfitting. *The journal of machine learning research* 15, 1 (2014), 1929–1958.
- [64] Allan Stisen, Henrik Blunck, Sourav Bhattacharya, Thor Siiger Prentow, Mikkel Baun Kjærgaard, Anind Dey, Tobias Sonne, and Mads Møller Jensen. 2015. Smart devices are different: Assessing and mitigating mobile sensing heterogeneities for activity recognition. In *Proceedings of the 13th ACM conference on embedded networked sensor systems*. 127–140.
- [65] Chi Ian Tang, Ignacio Perez-Pozuelo, Dimitris Spathis, Soren Brage, Nick Wareham, and Cecilia Mascolo. 2021. SelfHAR: Improving Human Activity Recognition through Self-training with Unlabeled Data. *arXiv preprint arXiv:2102.06073* (2021).
- [66] Chi Ian Tang, Ignacio Perez-Pozuelo, Dimitris Spathis, and Cecilia Mascolo. 2020. Exploring Contrastive Learning in Human Activity Recognition for Healthcare. *arXiv preprint arXiv:2011.11542* (2020).
- [67] Aaron Van den Oord, Yazhe Li, and Oriol Vinyals. 2018. Representation learning with contrastive predictive coding. *arXiv e-prints* (2018), arXiv–1807.
- [68] Laurens Van der Maaten and Geoffrey Hinton. 2008. Visualizing data using t-SNE. *Journal of machine learning research* 9, 11 (2008).
- [69] Ashish Vaswani, Noam Shazeer, Niki Parmar, Jakob Uszkoreit, Llion Jones, Aidan N Gomez, Łukasz Kaiser, and Illia Polosukhin. 2017. Attention is all you need. *Advances in neural information processing systems* 30 (2017).
- [70] Ivan Vulić, Edoardo Maria Ponti, Robert Litschko, Goran Glavaš, and Anna Korhonen. 2020. Probing pretrained language models for lexical semantics. *arXiv preprint arXiv:2010.05731* (2020).
- [71] Bram Wallace and Bharath Hariharan. 2020. Extending and analyzing self-supervised learning across domains. In *European Conference on Computer Vision*. Springer, 717–734.
- [72] Alex Wang, Amanpreet Singh, Julian Michael, Felix Hill, Omer Levy, and Samuel R Bowman. 2018. GLUE: A multi-task benchmark and analysis platform for natural language understanding. *arXiv preprint arXiv:1804.07461* (2018).
- [73] Matthew Willetts, Sven Hollowell, Louis Aslett, Chris Holmes, and Aiden Doherty. 2018. Statistical machine learning of sleep and physical activity phenotypes from sensor data in 96,220 UK Biobank participants. *Scientific reports* 8, 1 (2018), 1–10.
- [74] Yuzhe Yang and Zhi Xu. 2020. Rethinking the value of labels for improving class-imbalanced learning. *Advances in Neural Information Processing Systems* 33 (2020), 19290–19301.
- [75] Mi Zhang and Alexander A Sawchuk. 2012. USC-HAD: a daily activity dataset for ubiquitous activity recognition using wearable sensors. In *Proceedings of the 2012 ACM conference on ubiquitous computing*. 1036–1043.

## 8 APPENDIX

Table 6. Best performing hyperparameters for Multi-task self-supervision for each target dataset.

Dataset	lr	L2 reg.	class. lr	class. L2 reg.	F1-score (mean)	F1-score (std)
HHAR	0.0005	0.0001	0.0001	0.00001	58.1	1.06
Myogym	0.0005	0.00001	0.0005	0.0001	39.89	0.98
Wetlab	0.001	0.0001	0.0005	0	24.16	0.48
Mobiact	0.001	0.00001	0.0005	0	72.91	0.99
Motionsense	0.001	0	0.0001	0.00001	84.74	1.14
USC-HAD	0.0005	0.00001	0.0005	0.0001	51.37	2.43
Daphnet	0.001	0.0001	0.0005	0	51.16	1
MHEALTH	0.0005	0.00001	0.0005	0.0001	45.49	1.27
PAMAP2	0.001	0	0.0001	0.00001	52.24	1.98

Table 7. Best performing hyperparameters for Masked Reconstruction for each target dataset.

Dataset	head	layers	mask%	warmup	class. lr	class. L2 reg.	F1-score (mean)	F1-score (std)
HHAR	8	6	10	80000	0.0005	0.0001	55.04	2.58
Myogym	8	3	40	80000	0.0005	0.0001	25.29	0.68
Wetlab	8	6	10	80000	0.0005	0.0001	21.23	0.31
Mobiact	8	6	70	60000	0.0005	0	54.17	1.38
Motionsense	8	4	50	60000	0.0001	0	75.72	1.88
USC-HAD	8	4	70	80000	0.0005	0.0001	45.09	0.92
Daphnet	8	4	50	60000	0.0005	0.0001	52.51	1.01
MHEALTH	8	6	40	40000	0.0005	0.00001	47.04	0.61
PAMAP2	8	5	60	60000	0.0005	0	55.12	0.96

Table 8. Best performing hyperparameters for CPC for each target dataset.

Dataset	k	lr	L2 reg.	class. lr	class. L2 reg.	F1-score (mean)	F1-score (std)
HHAR	48	0.0005	0.0001	0.0001	0.00001	58.1	1.06
Myogym	48	0.0005	0.00001	0.0005	0.0001	39.89	0.98
Wetlab	48	0.001	0.0001	0.0005	0	24.16	0.48
Mobiact	64	0.001	0.00001	0.0005	0	72.91	0.99
Motionsense	32	0.001	0	0.0001	0.00001	84.74	1.14
USC-HAD	48	0.0005	0.00001	0.0005	0.0001	51.37	2.43
Daphnet	48	0.001	0.0001	0.0005	0	51.16	1
MHEALTH	48	0.0005	0.00001	0.0005	0.0001	45.49	1.27
PAMAP2	32	0.001	0	0.0001	0.00001	52.24	1.98

This manuscript is under review. Please write to harishkashyap@gatech.edu for up-to-date information.

Table 9. Best performing hyperparameters for Autoencoder for each target dataset.

Dataset	kernel_size	lr	wd	class. lr	class. L2 reg.	F1-score (mean)	F1-score (std)
HHAR	11	0.001	0	0.0001	0.00001	54.25	2.04
Myogym	9	0.001	0.00001	0.0005	0.00001	35.45	0.49
Wetlab	11	0.0005	0.0001	0.0001	0	25.75	1.03
Mobiact	9	0.0005	0.0001	0.0005	0.0001	68.69	0.56
Motionsense	11	0.0005	0.0001	0.0001	0	80.7	1.66
USC-HAD	7	0.001	0	0.0005	0.0001	51.32	2.16
Daphnet	9	0.001	0.00001	0.0005	0.00001	53.05	0.85
MHEALTH	7	0.0001	0	0.0005	0.00001	39.2	1.58
PAMAP2	11	0.001	0	0.0005	0	56.88	2.04

Table 10. Best performing hyperparameters for DeepConvLSTM for each target dataset.

Dataset	lr	wd	F1-score (mean)	F1-score (std)
HHAR	0.0005	0	54.39	2.28
Myogym	0.0005	0.00001	39.9	1.05
Wetlab	0.001	0	31	0.68
Mobiact	0.001	0.00001	82.21	0.69
Motionsense	0.0001	0.0001	84.56	0.85
USC-HAD	0.0005	0.0001	53.64	0.51
Daphnet	0.0001	0.00001	53.68	2.58
MHEALTH	0.0005	0	45.91	0.89
PAMAP2	0.001	0	51.22	1.91

Table 11. Best performing hyperparameters overall, across all target datasets.

Approach	Best overall parameters
Multi-task	lr=0.0003, l2 reg.=0.0005, class. lr=0.0003, class. l2 reg.=0
Masked recons.	head=8, layers=6, mask%=10, warmup=80000, class. lr=0.0005, class. l2 reg.=0.0001
CPC	lr=0.0001, l2 reg.=0.00001, kernel_size=3, k=64, bs=256, class. lr=0.0005, class. l2 reg.=0
Autoencoder	lr=0.001, wd=0.00001, kernel_size=9, class. lr=0.0005, class. l2 reg.=0.00001

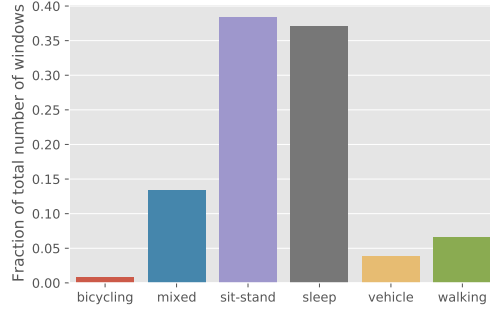


Fig. 14. The class composition of the Capture-24 train dataset, demonstrating that it is imbalanced. Sleep and sit-stand comprise around 75% of the total dataset, whereas bicycling only consists of 0.78% of the train data.

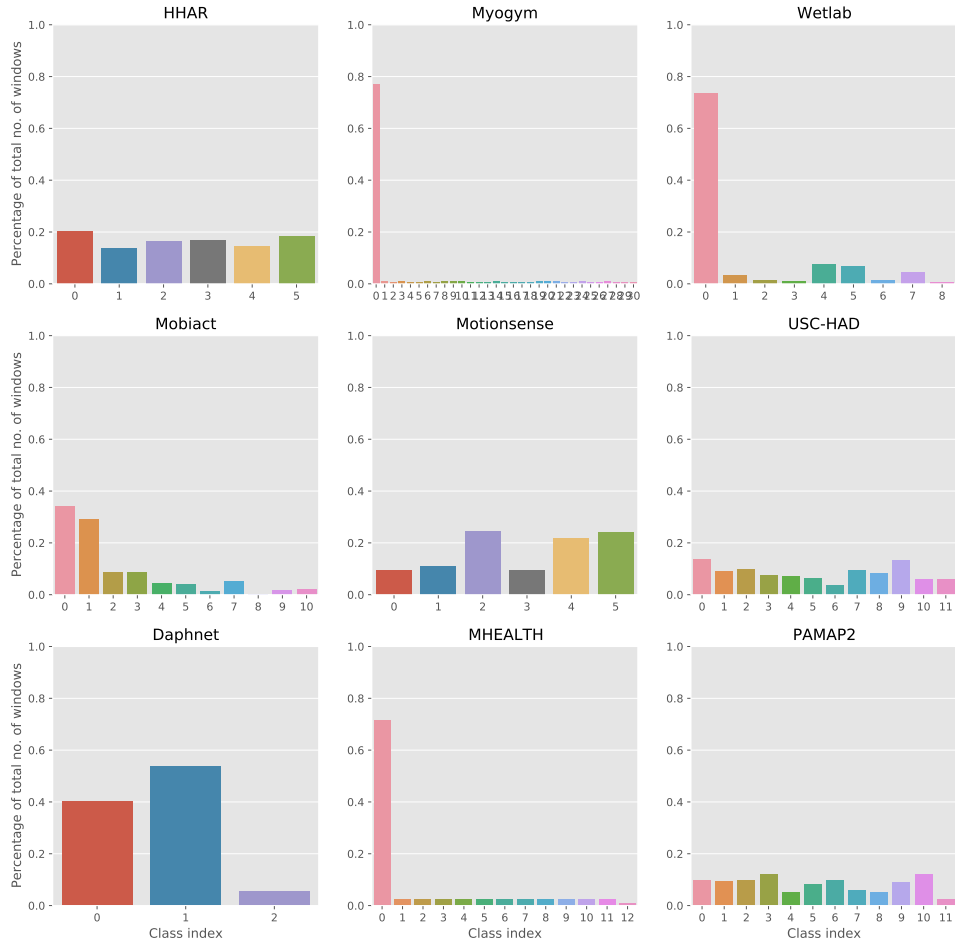


Fig. 15. The class composition of all target datasets.

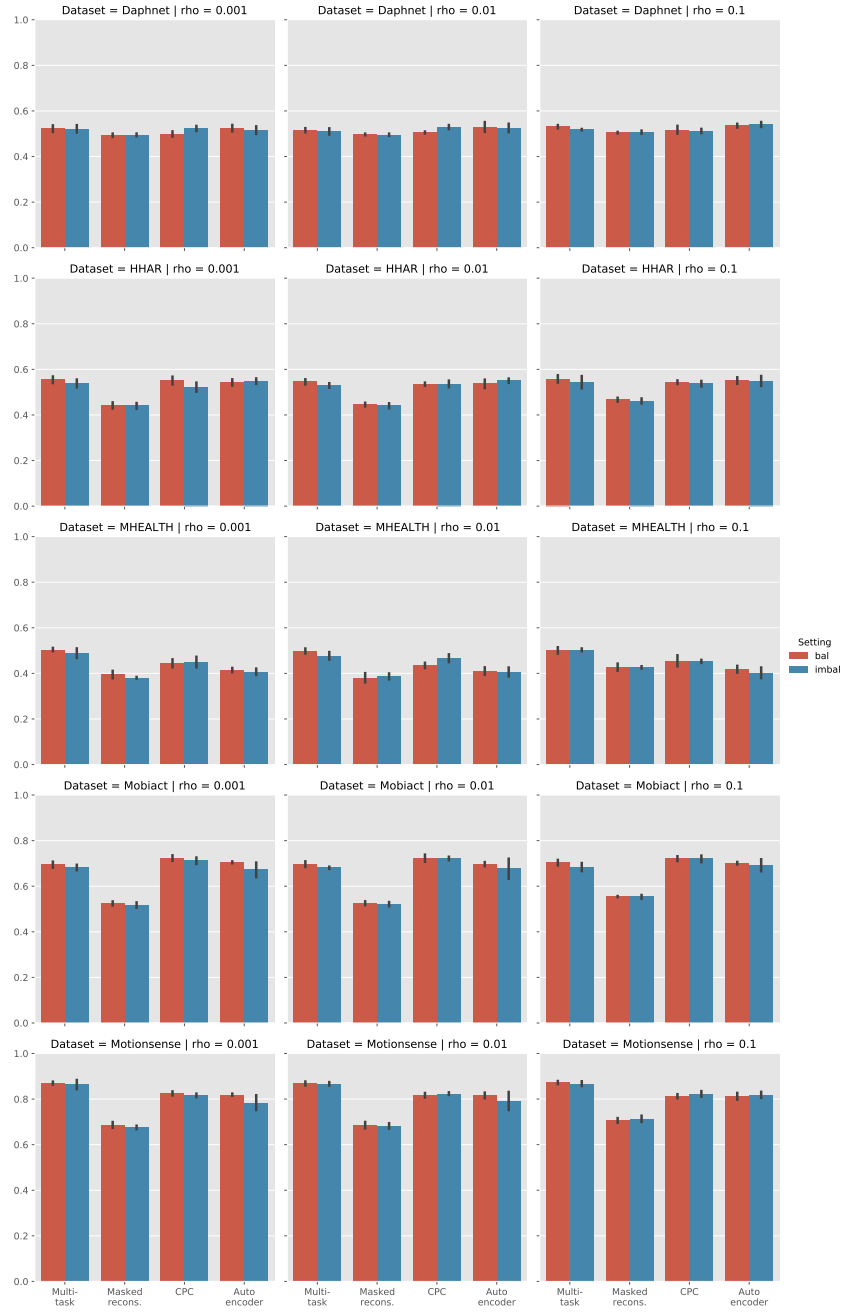


Fig. 16. Impact of the source dataset imbalance on the activity recognition performance - Part 1.

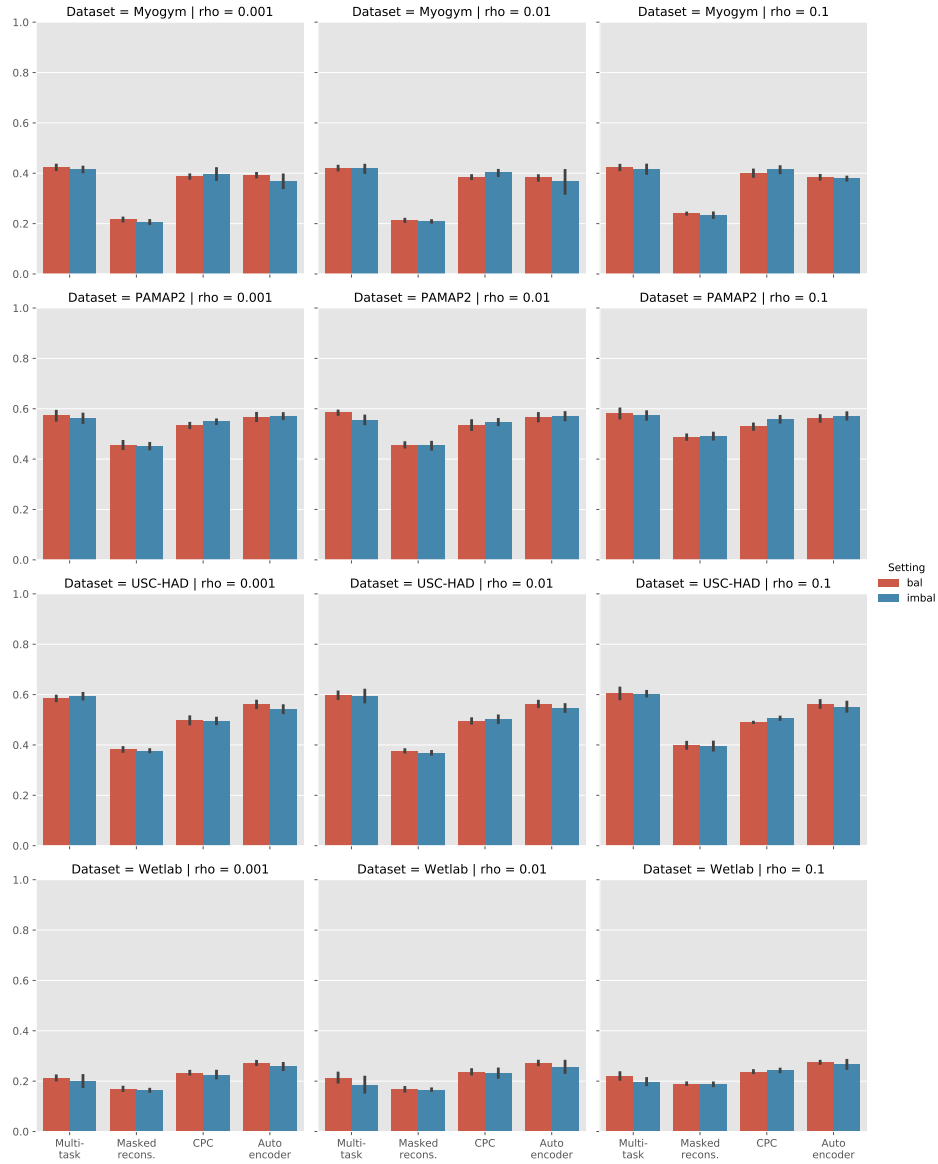


Fig. 17. Impact of the source dataset imbalance on the activity recognition performance - Part 2.

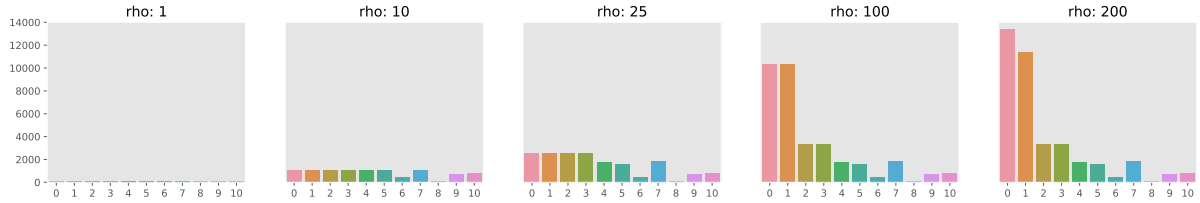


Fig. 18. Visualizing the class distributions for various values of the imbalance ratio  $\rho$  in the train split of the first fold of the Mobiact dataset. The maximum number of allowed windows is dependent on the size of the rarest class and  $\rho$ . For  $\rho \in \{1, 10, 25, 100, 200\}$ , the final size of the training dataset is  $\{1.1k, 9.3k, 17.5k, 34.5k, 38.7k\}$  windows respectively.

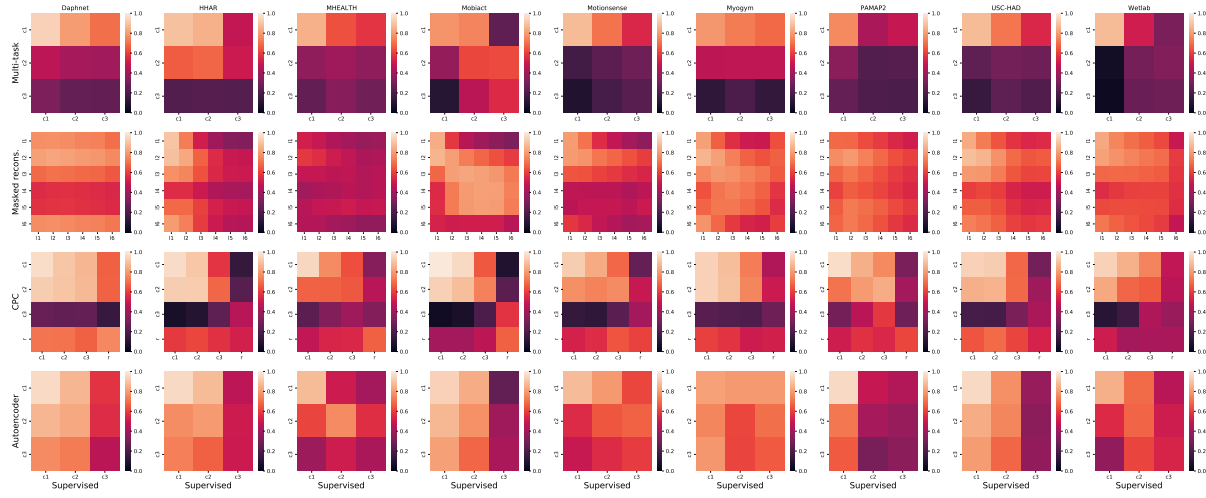


Fig. 19. Similarity of the learned representations to supervised learning.

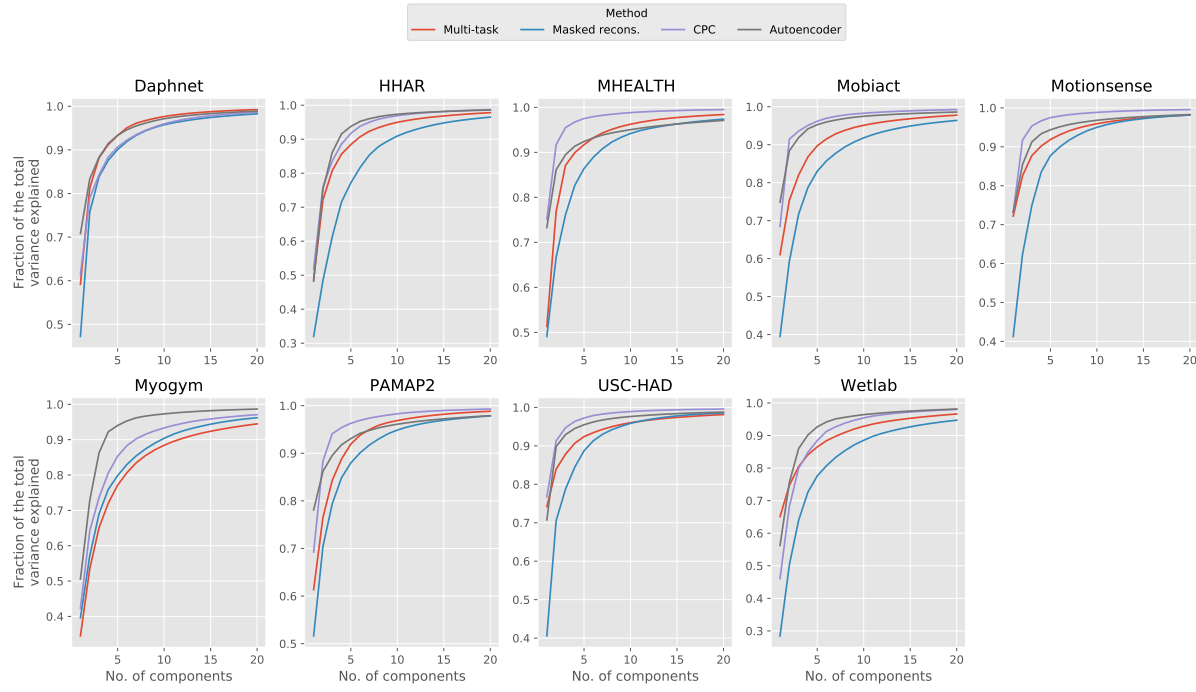


Fig. 20. Implicit dimensionality of the self-supervised approaches for individual target datasets.

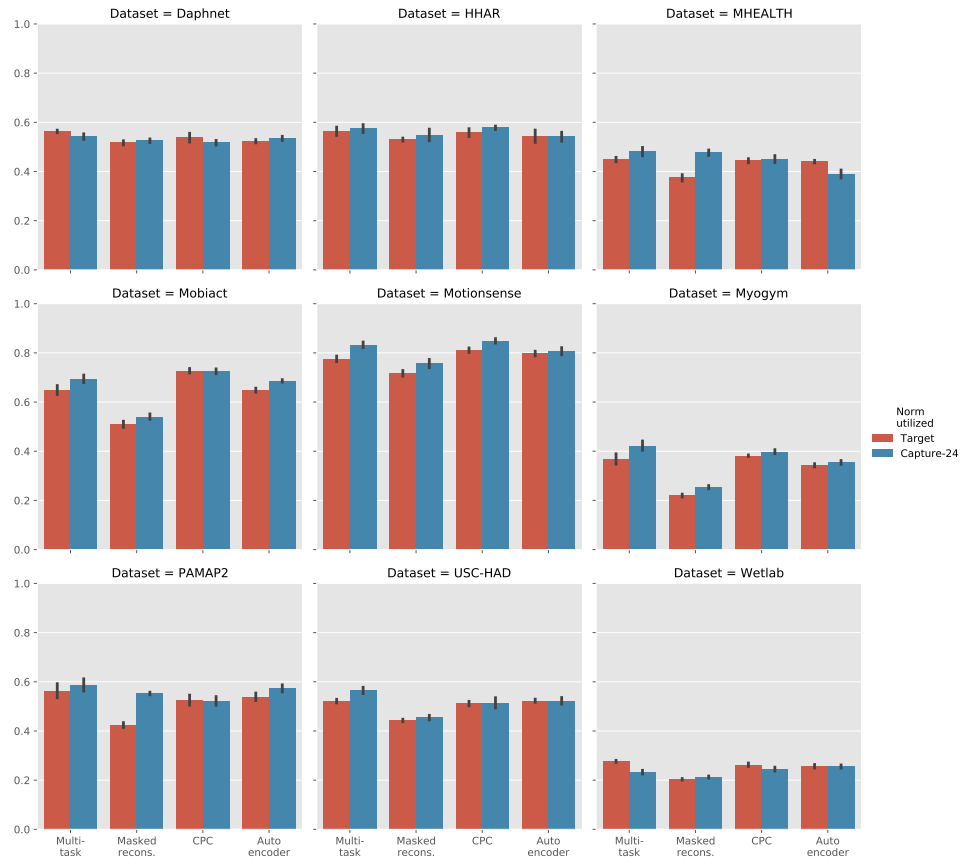


Fig. 21. Activity recognition performance when utilizing either the source dataset means and variances, or the target dataset statistics.